Finite Element and Finite Difference Methods for Maxwell's Equations in Metamaterials

By
Isaac Stallcup

A THESIS

submitted to

Oregon State University

Honors College

in partial fulfillment of
the requirements for the
degree of

Honors Baccalaureate of Science in Mathematics (Honors Scholar)
Honors Baccalaureate of Science in Computer Science
(Honors Scholar)

Presented March 15, 2018
Commencement June 2018

AN ABSTRACT OF THE THESIS OF

Isaac Stallcup for the degree of Honors Baccalaureate of Science in Mathematics and Computer Science presented on March 15, 2018. Title:
Finite Element and Finite Difference Methods for Maxwell's Equations in Metamaterials

Abstract approved:

Vrushali Bokil

In this thesis, we consider Maxwell's Equations and their numerical discretization using finite difference and finite element methods. We first describe Maxwell's equations in linear dielectrics and then present finite difference and finite element methods for this case. We then describe Maxwell's equations in linear metamaterials using the Lorentz and Drude models. Finally, we construct a finite element method for Maxwell's Equations in a Lorentz metamaterial. An exact solution of the model system, involving both partial differential equations of the Maxwell system and ordinary differential equations describing the response of the Lorentz metamaterial, is constructed. Finite element simulations are then performed and tested against this exact solution to demonstrate the accuracy of the method.

Key Words: Maxwell's Equations, Linear dielectrics, Finite Element Methods, Finite Difference Methods, Lorentz Metamaterials

Corresponding e-mail address: isaac.stallcup@gmail.com, or stallcui@oregonstate.edu

Finite Element and Finite Difference Methods for Maxwell's Equations in Metamaterials

By
Isaac Stallcup

A THESIS

submitted to

Oregon State University

Honors College

in partial fulfillment of
the requirements for the
degree of

Honors Baccalaureate of Science in Mathematics (Honors Scholar)
Honors Baccalaureate of Science in Computer Science
(Honors Scholar)

Presented March 15, 2018
Commencement June 2018

Honors Baccalaureate of Science in Mathematics and Computer Science project of Isaac Stallcup presented on March 15, 2018

APPROVED:

Vrushali Bokil, Mentor, representing Mathematics

Nathan Gibson, Committee Member, representing Mathematics

Elaine Cozzi, Committee Member, representing Mathematics

Toni Doolen, Dean, Oregon State University Honors College

I understand that my project will become part of the permanent collection of Oregon State University Honors College. My signature below authorizes release of my project to any reader upon request.

Isaac Stallcup, Author

Finite Element and Finite Differece Methods for Maxwell's Equations in Metamaterials

Isaac Stallcup

March 16, 2018

Contents

List of Figures

List of Symbols

N The number of intervals or elements in which Ω is discretized into.

Γ_e Electric damping frequency.

Γ_m Magnetic damping frequency.

ϵ_0 Permittivity.

μ Free-space permeability.

μ_0 Permeability.

ω_{e0} Electric resonance frequency.

ω_{m0} Magnetic resonance frequency.

ω_{pe} Electric plasma frequency.

ω_{pm} Magnetic plasma frequency.

ε Free-space permittivity.

$\vec{B}$ Magnetic flux density.

$\vec{D}$ Electric flux density.

$\vec{E}$ Electric field.

$\vec{H}$ Magnetic field.

$\vec{J}$ Polarization current density.

$\vec{K}$ Magnetization current density.

$\vec{M}$ Magnetization.

$\vec{P}$ Electric polarization.

h Mesh step size.

Acknowledgements

Thank you to my mentor, Dr. Vrushali Bokil, without whom none of this paper would have been possible! Thank you also to Dr. Tevian Dray, who inspired me almost five years ago to continue to pursue a degree in mathematics. Last but the opposite of least, I'd like to thank my wonderful fiancee, Kiana Murray (soon to be Stallcup), whose support and companionship has kept me sane and healthy throughout the process of this thesis.

1 Introduction

Maxwell's equations are a system of vector partial differential equations (PDEs) describing how electricity and magnetism interact and behave in a material. Developed in the 19th century by physicist James Clerk Maxwell [3], they are the culmination of hundreds (if not thousands) of years' study, experimentation and thought on the relationship between the phenomena of electricity and magnetism.

Fundamentally, Maxwell's equations provide a mathematical toolkit through which the response of a material to electric and magnetic fields can be understood, modeled and predicted. Virtually all electronic technology developed today owes its existence to this set of four equations, from radio transmissions to computing. Astronomy, engineering, computer science and physics are just four examples of entire fields that use Maxwell's equations to help understand electromagnetic wave propagation in different frequency ranges. In short, they are a cornerstone of classical physics.

In the 150+ years since their discovery, computing technology has advanced quite considerably. Computational electromagnetics is a field that combines physics, mathematics and computer science to use computational techniques to solve problems described by Maxwell's equations. Doing so involves developing and using highly efficient classes of approximations to Maxwell's equations, since in most cases it is impossible to find exact solutions. These classes of methods are called numerical methods, and their study is the field of Numerical Analysis. Two such numerical methods, Finite Difference Methods and Finite Element Methods, will be examined in this thesis.

The first group of numerical methods, Finite Difference Methods, rely on approximating derivatives by finite differences obtained through Taylor approximations [4]. The second group of methods, Finite Element Methods, are based on approximating an integral reformulation of the model differential equations [4].

Finite Difference and Finite Element methods will be examined that model a variety of electromagnetic problems in one dimension. First the theoretical aspects of the methods will be developed, after which they will be computationally applied to several example problems in order to demonstrate their effectiveness and accuracy. In particular, we focus on the cases of wave propagation in linear dielectrics and linear metamaterials.

Among these problems is one examining electrical wave propagation in metamaterials. First imagined in 1968 by Russian physicist Victor Veselago [2], a metamaterial is an artificially structured composite material whose interaction with electromagnetic waves do not resemble that of materials found in nature. This unusual interaction is due to negative values for the material properties of permittivity and permeability, which are themselves artifacts of the molecular structure of the metamaterial.

The result of the simultaneous negativity of permeability and permittivity allows for novel properties. One such property is the reversing of the Doppler effect [2]. The Doppler effect

is perhaps best known as the effect responsible for the change in tone as an ambulance or fire engine passes by. When the siren is approaching, the sound waves are compressed as they travel, causing the pitch to increase. As the siren recedes, the sound waves are stretched, causing the pitch to decrease. The reversal of this Doppler effect means that as an electrical wave travels through a metamaterial, its frequency decreases as the wave source moves closer [2].

Another possibility that metamaterials introduce is that of optical cloaking. Long a staple of science fiction and fantasy, cloaking devices hide objects from some or all portions of the electromagnetic spectrum [2]. The general idea is to guide electromagnetic waves (potentially including visible light) around objects, therefore removing their ability to reflect from the object and thus allowing the object to escape detection.

Despite their intriguing nature and potential use, metamaterials remained unknown for 30 years after they were proposed in theory. It took Veselago's work until 2000 to come into physical being, when a team lead by D.R. Smith constructed one such material using copper split ring resonators [5]. Since then, metamaterials have been a topic of much research and thought.

Constructing a numerical method loosely follows the following blueprint: first, the system of Maxwell's equations and equations for the metamaterial response are reduced to the dimension of the problem (in the case of this thesis, one spatial dimension). Then the problem is discretized; this essentially breaks up the domain of the problem into a finite set of points or elements, instead of a continuous domain. Additionally, the time domain is discretized into discrete time steps. Finally finite differences or the finite element method are used to construct a discrete approximation. The result is a linear system of equations that has to be solved at every time iteration in the finite element method, whereas in the finite difference method that we consider, explicit update equations are set up to discretely update the solution in space and time.

The outline of the thesis is as follows. In Section 2, we describe Maxwell's equations in linear dielectrics. In Section 3, we discuss the Finite Difference Time Domain or Yee scheme, and provide examples of its application in 1D to linear dielectrics. In Section 4, we discuss the Finite Element Method, its development, and application to linear dielectrics. In Section 5, we discuss the case of Maxwell's equations in Drude- and Lorentz-type metamaterials, and apply the Finite Element Method to a Lorentz-type metamaterial after developing an exact solution. Finally, Section 6 provides conclusions and a brief discussion.

The programming language and associated software MATALB is used in this thesis to carry out numerical simulations. Code for each simulation can be found in Section 7 of this document.

2 Maxwell's Equations in Linear Dielectrics

We begin with Maxwell's Equations in a material $\Omega \subseteq \mathbb{R}^3$. These are a system of vector partial differential equations given as

Maxwell's Equations

$$\textbf{Faraday's Law} \qquad \frac{\partial \vec{B}}{\partial t} = -\nabla \times \vec{E}, \tag{2.1a}$$

$$\textbf{Maxwell-Ampére Law} \qquad \frac{\partial \vec{D}}{\partial t} = \nabla \times \vec{H} - \vec{J}, \tag{2.1b}$$

$$\textbf{Gauss's Law} \qquad \nabla \cdot \vec{B} = 0, \tag{2.1c}$$

$$\textbf{Gauss-Poisson Law} \qquad \nabla \cdot \vec{D} = \rho. \tag{2.1d}$$

$$\tag{2.1e}$$

In System 2.1, $\vec{D}$ represents the electric flux density, $\vec{E}$ represents the electric field, $\vec{B}$ represents the magnetic flux density and $\vec{H}$ represents the magnetic field. All field variables are functions of time t and space $\vec{x} = (x, y, z) \in \mathbb{R}^3$. The current density $\vec{J}$ and the charge density ρ are related by the continuity equation

$$\frac{d\rho}{dt} + \nabla \cdot \vec{J} = 0. \tag{2.2}$$

These classical equations provide a total of twelve unknown quantities, but only eight equations in which to solve for them, meaning that to find concrete solutions we must append to Maxwell's equations several other physical laws governing the response of the material, called the constitutive laws.

Constitutive laws govern the behavior of electromagnetic waves in different media; for linear dielectric media, such as a vacuum, the constitutive laws that pertain to Maxwell's equations are

$$\vec{D} = \varepsilon \vec{E}, \tag{2.3}$$

$$\vec{B} = \mu \vec{H}, \tag{2.4}$$

with the material-dependent parameters ε, the frequency-independent electric permittivity, and μ, the frequency-independent magnetic permeability. We consider linear dielectrics in which ε and μ are constants. In metamaterials, these are not constants, but instead functions of the angular frequency of a wave propagating through the material. When substituted into Equations (2.1b) and (2.1a), the resulting pair of equations relates $\vec{E}$ and $\vec{H}$ directly as seen

through the equations:

$$\begin{aligned} \textbf{Faraday's Law} \qquad & \mu\frac{\partial \vec{H}}{\partial t} = -\nabla \times \vec{E}, \\ \textbf{Maxwell-Ampére Law} \qquad & \varepsilon\frac{\partial \vec{E}}{\partial t} = \nabla \times \vec{H}. \end{aligned} \tag{2.5}$$

These are called the curl equations of the Maxwell system. From (2.1c) and (2.1d) we can also glean two conditions that must be satisfied for these adapted forms, namely that

$$\begin{aligned} \nabla \cdot (\varepsilon \vec{E}) &= \rho, \\ \nabla \cdot (\mu \vec{H}) &= 0, \end{aligned}$$

where ρ is some given charge density.

These conditions, combined with system (2.5) are then in a form with which we can describe the behavior of the electric and magnetic fields in a linear dielectric when ε and μ are constants. Given some initial conditions $\vec{E}_0$ and $\vec{H}_0$ and additional boundary conditions, we can then simulate the changes in the system from the initial state as it moves through time, modeling the propagation of electromagnetic waves in the dielectric.

In the case when ε and μ are frequency dependent, additional equations have to be added to the Maxwell system. This happens in the case of metamaterials and is discussed in Section 4. We consider problems in one spatial dimension. We first discuss reducing the Maxwell system to two spatial dimensions. Reducing to two dimensions gives rise to two separate decoupled systems of three equations each, called the **Transverse Electric** and **Transverse Magnetic** modes [4].

2.1 Dimensional Reduction

Though existing in three dimensions classically, it is useful to reduce Maxwell's equations down into two or one dimensions for problems that have special properties and symmetries. The process of doing so relies on the curl equations given in (2.5).

To begin this process, we first write the Maxwell curl equations in scalar form. Each field variable $\vec{V} = \vec{E}, \vec{H}, \vec{B}$, and $\vec{D}$ has three components that we denote $\vec{V} = (V_x, V_y, V_z)$ with

V_x, V_y, V_z functions of time and space, so the system can be written as

$$\begin{aligned}
\mu\frac{\partial H_x}{\partial t} &= -\left(\frac{\partial E_z}{\partial y} - \frac{\partial E_y}{\partial z}\right), \\
\mu\frac{\partial H_y}{\partial t} &= -\left(\frac{\partial E_x}{\partial z} - \frac{\partial E_z}{\partial x}\right), \\
\mu\frac{\partial H_z}{\partial t} &= -\left(\frac{\partial E_y}{\partial x} - \frac{\partial E_x}{\partial y}\right); \\
\varepsilon\frac{\partial E_x}{\partial t} &= \left(\frac{\partial H_z}{\partial y} - \frac{\partial H_y}{\partial z}\right), \\
\varepsilon\frac{\partial E_y}{\partial t} &= \left(\frac{\partial H_x}{\partial z} - \frac{\partial H_z}{\partial x}\right), \\
\varepsilon\frac{\partial E_z}{\partial t} &= \left(\frac{\partial H_y}{\partial x} - \frac{\partial H_x}{\partial y}\right).
\end{aligned} \tag{2.6}$$

Once these curl operators have been expanded, it is possible to set certain components of $\vec{E}$ and $\vec{H}$ to zero in order to represent that they do not exist in the chosen dimension. In addition, we assume that all field components and properties do not change along some given dimension. This process is detailed for reduction to both two and one spatial dimensions in the following sections.

2.1.1 Reduction to Two Dimensions

Reducing Maxwell's equations to two dimensions at its heart involves assuming that both electric and magnetic fields have no dependence on one of the three classical Cartesian dimensions x, y, z. However, to satisfy the result in system (2.6), two cases, or modes, present themselves.

In the first mode, we can define the electric field $\vec{E}$ to propagate in the x and y directions, while not changing in the z direction. As a result of Maxwell's equations, we must then have the magnetic field propagate in a way that is perpendicular to the $x-y$ plane, the z direction, while not changing properties in z. Mathematically this is done by setting $E_z = 0$, and $H_x = H_y = 0$ and assuming all derivatives in the z direction are 0. Plugging these values into system (2.6) then gives the Transverse Electric mode of Maxwell's equations. This is a set of three expressions, shown in system (2.7) below.

The second mode defines $\vec{H}$ to propagate in the x and y directions, while not changing properties in z ; and as a result $\vec{E}$ propagates in the z direction while not changing in z. In system (2.6), $H_z = 0$ and $E_x = E_y = 0$. Substituting into (2.6) then gives the Transverse Magnetic mode. This is shown in system (2.8).

The choice of nonzero terms in $\vec{E}$ & $\vec{H}$, dictated by Maxwell's equations, is responsible for

one of their most important results: that the *orientation* in space of $\vec{E}$ and $\vec{H}$ is mutually orthogonal. These two sets of equations for $\vec{E}$ and $\vec{H}$ are then ready to be discretized to create numerical methods.

The complete reduction of Maxwell's equations to 2D from their 3D versions is detailed below. For the Transverse Electric mode, set $E_z = 0$, and $H_x = H_y = 0$ and $\frac{d}{dz} = 0$ in system (2.5). This then gives

$$\nabla \times \vec{H} = \begin{vmatrix} \hat{x} & \hat{y} & \hat{z} \\ \frac{\partial}{\partial x} & \frac{\partial}{\partial y} & 0 \\ 0 & 0 & H_z \end{vmatrix} = \hat{x}\left(\frac{\partial H_z}{\partial y} - 0\right) + \hat{y}\left(0 - \frac{\partial H_z}{\partial x}\right) + \hat{z}\,(0-0) = \hat{x}\left(\frac{\partial H_z}{\partial y}\right) - \hat{y}\left(\frac{\partial H_z}{\partial x}\right),$$

and

$$\nabla \times \vec{E} = \begin{vmatrix} \hat{x} & \hat{y} & \hat{z} \\ \frac{\partial}{\partial x} & \frac{\partial}{\partial y} & 0 \\ E_x & E_y & 0 \end{vmatrix} = \hat{x}\,(0-0) + \hat{y}\,(0-0) + \hat{z}\left(\frac{\partial E_y}{\partial x} - \frac{\partial E_x}{\partial y}\right) = \hat{z}\left(\frac{\partial E_y}{\partial x} - \frac{\partial E_x}{\partial y}\right).$$

IN the above, $\hat{x}$, $\hat{y}$ and $\hat{z}$ are unit vectors in the x, y and z directions respectively. Substituting the above formulas back into the curl equations (2.5) then results in the vector system

$$\begin{aligned} \varepsilon \frac{\partial \vec{E}}{\partial t} &= \hat{x}\left(\frac{\partial H_z}{\partial y}\right) - \hat{y}\left(\frac{\partial H_z}{\partial x}\right), \\ \mu \frac{\partial \vec{H}}{\partial t} &= \hat{z}\left(\frac{\partial E_x}{\partial y} - \frac{\partial E_y}{\partial x}\right), \end{aligned}$$

with $\vec{E} = (E_x, E_y, 0)$ and $\vec{H} = (0, 0, H_z)$. Separating out E_x and E_y from $\vec{E}$, we can then restate the system in scalar form as

$$\begin{aligned} \varepsilon \frac{\partial E_x}{\partial t} &= \frac{\partial H_z}{\partial y}, \\ \varepsilon \frac{\partial E_y}{\partial t} &= -\frac{\partial H_z}{\partial x}, \\ \mu \frac{\partial H_z}{\partial t} &= \frac{\partial E_x}{\partial y} - \frac{\partial E_y}{\partial x}. \end{aligned}$$

This system of equations is called the Transverse Electric Mode in two spatial dimensions.

$$\text{Transverse Electric (TE) Mode} \begin{cases} \mu \dfrac{\partial H_z}{\partial t} = \dfrac{\partial E_x}{\partial y} - \dfrac{\partial E_y}{\partial x}, \\ \varepsilon \dfrac{\partial E_y}{\partial t} = -\dfrac{\partial H_z}{\partial x}, \\ \varepsilon \dfrac{\partial E_x}{\partial t} = \dfrac{\partial H_z}{\partial y}. \end{cases} \tag{2.7}$$

We can similarly obtain the Transverse Magnetic mode as

$$\text{Transverse Magnetic (TM) Mode} \begin{cases} \varepsilon \dfrac{\partial E_z}{\partial t} = \dfrac{\partial H_x}{\partial y} - \dfrac{\partial H_y}{\partial x}, \\ \mu \dfrac{\partial H_y}{\partial t} = -\dfrac{\partial E_z}{\partial x}, \\ \mu \dfrac{\partial H_x}{\partial t} = \dfrac{\partial E_z}{\partial y}. \end{cases} \tag{2.8}$$

We note that in this process of reduction we lose one of Gauss' Laws. In the TE mode, the divergence of the magnetic field is lost. We only have $\text{div}(\epsilon \vec{E}) = \rho$ in this mode, while in the TM mode the divergence of the electric field is lost. We only retain $\text{div}(\mu \vec{H}) = 0$.

2.1.2 Reduction to One Dimension

Problems involving Maxwell's equations can be represented in one spatial dimension for each of $\vec{E}$ and $\vec{H}$; essentially becoming one dimensional waves that, in the physical world, propagate in time.

A real-world example of a 1D wave propagating in time is that of a rope held by two people, one person at each end. If one of the holders raises then lowers the rope sharply, the "wave" formed by the motion will travel along the rope, eventually reaching the other holder.

Mathematically, a 1-D vector field $\vec{E}$ only has one of its components E_x, E_y, E_z as non-zero; yet the choice of nonzero component is far from arbitrary. The selection is motivated by the curl equations in (2.5). These are again expanded to the form given in (2.6).

To reduce the problem to one dimension, first set E_z, H_x, and $H_y = 0$, reducing each part of the problem to the two dimensional TE mode. After reducing to two dimensions, further reduce to one dimension by choosing $E_x = 0$, canceling all E_x terms in the two-dimensional TE mode and all derivatives in the y direction to zero.

This is an arbitrary choice to suit the dimension of the problem; it is just as easy to choose E_y to be zero resulting in a different but similar set of equations. The choice of $E_x = 0$, along with $\frac{d}{dy} = 0$, then gives the resulting pair of equations

$$\mu \frac{\partial H_z}{\partial t} = -\frac{\partial E_y}{\partial x}, \qquad \varepsilon \frac{\partial E_y}{\partial t} = -\frac{\partial H_z}{\partial x}. \tag{2.9}$$

We note that in this 1D reduction we lose both Gauss laws in the sense that the Gauss laws become decoupled from the system in (2.9). Thus, working with this pair in one spatial dimension and time, we can now move on to detailing the process of discretizing the spatial and temporal domains.

3 The Finite Difference Time Domain Method

Finite difference methods encompass a class of numerical techniques to approximate ordinary and partial derivatives. In this case, we require a finite difference operation that is then used to approximate derivatives in both time ($\frac{\partial E}{\partial t}, \frac{\partial H}{\partial t}$) and space ($\frac{\partial E}{\partial x}, \frac{\partial H}{\partial x}$). A relatively simple finite difference method that accomplishes this is the forward difference approximation, which can be used to approximate derivatives.

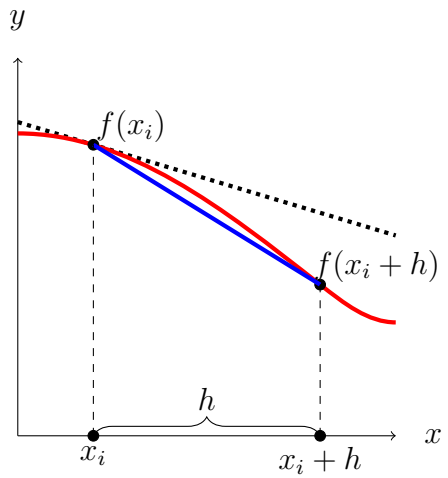

Figure 3.1: An example of a Forward Difference approximation of $\frac{\partial f(x_i)}{\partial x}$. Note the tangent line, shown as a dashed line, and how the approximate line (shown as a blue line) differs.

The derivative of some arbitrary function f at a point x_i is defined as

$$\frac{\partial f(x_i)}{\partial x} = \lim_{h \to 0} \left[\frac{f(x_i + h) - f(x_i)}{h} \right]. \tag{3.1}$$

The exact value of the derivative is reached in the limit when the space between sample points, h, is infinitesimally small as it approaches zero.

A forward difference bears a striking resemblance to the limit's numerator in 3.1; it is defined as

$$\frac{f(x_i + h) - f(x_i)}{h} \tag{3.2}$$

for some small $h > 0$.

A forward finite difference can be used to approximate the derivative of a function f at a point x_i; to do so, substitute the forward difference; the result is

$$\frac{\partial f(x_i)}{\partial x} \approx \frac{f(x_i + h) - f(x_i)}{h}. \tag{3.3}$$

This difference is the slope of a secant line drawn between the original point $f(x_i)$ and the point $f(x_i + h)$, which approximates the slope of the tangent line to f at a point x_i.

From the definition in Equation (3.1), we can surmise that as h becomes smaller, the slope of the secant line given by the forward difference gives an increasingly accurate approximation of the slope of the tangent line as $h \to 0$.

3.1 Spatial Discretization

When reduced to one dimension, as reviewed in Section 2.1, Maxwell's equations model the propagation of two perpendicularly oriented waves; one magnetic and one electric. A well-known finite difference method for Maxwell's equations is the Yee scheme [6], assembled through the application of centered differences in both time and space by a process of staggering electric and magnetic fields in space and time. In order to construct this scheme, first the domain in both time and space must undergo discretization.

3.1.1 Mesh Construction

Discretization is the process of approximating a continuous domain and functions by discrete meshes and fields, respectively. One simple example, which will be shown here, is choosing a set of points along a line that serve as a representation, or approximation, of the line itself.

In the case of finite difference methods (in both one and two dimensions), discretization takes the form of choosing points along the axis (in this case the x-axis),

We first choose N, the number of sub-intervals into which the domain $\Omega \subseteq \mathbb{R}$ will be divided into. Define the set of distinct points $\{x_1, x_2, \ldots, x_{N-1}, x_N\}$ such that $[x_1, x_2] \cup [x_2, x_3] \cup \ldots \cup [x_{N-1}, x_N] = \Omega$ such that the intersection of any two intervals is either empty or comprises of a common endpoint of the intervals. This set of points is also called a mesh. Define the mesh step sizes associated with the interval $[x_j, x_{j+1}]$ as $h_j = x_{j+1} - x_j$. A non-uniform mesh is a mesh such that at least one h_j is not equal to the others, as can be seen in Figure 3.2.

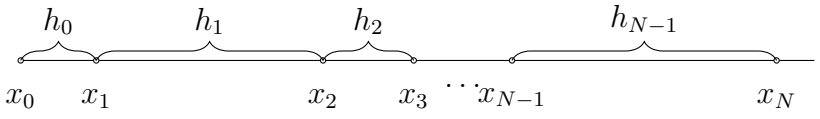

Figure 3.2: Non-Uniform Mesh

A mesh is called a uniform mesh if the mesh step sizes h_j are equal for all mesh points. In this case the step size is referred to as h. This step size is defined as $(x_{j+1} - x_j) = h_j = h \; \forall \, j \in [1, N]$. An example of this is given in Figure 3.3.

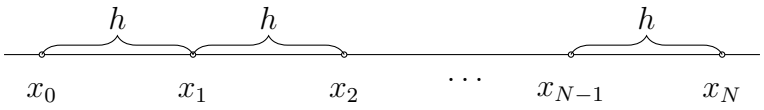

Figure 3.3: Uniform mesh. Each grid point is equally spaced every h units along the domain Ω.

In this case, $x_j = x_0 + jh \; \forall \; j = 1, 2, \ldots, N$.

3.1.2 Staggering of Electric and Magnetic Fields

In order to accurately model Maxwell's equations, we introduce separate meshes for the discretization of E and H. We denote the E mesh as the *primary* mesh, and the mesh for H as the *staggered* or *dual* mesh. The mesh nodes for the staggered mesh are located between points on the primary mesh, as seen in Figure 3.4. In a uniform mesh, the staggered mesh points are spaced halfway between those of the primary mesh.

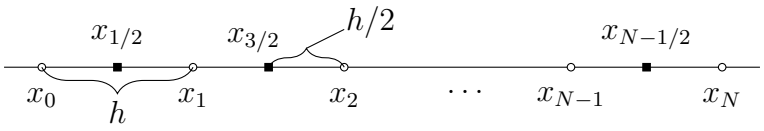

Figure 3.4: Primary and Staggered Meshes; with white circles representing primary grid points and black squares for staggered mesh points

In the numerical discretization of the system, values of E and H are only given at their respective mesh points; the same holds for values in time.

The discretization in terms of time shares this staggered approach; define $\Delta t > 0$ to be the time step, and discrete time points

$$t_n = n\Delta t, \text{ for } n \in N \text{ on the primary mesh}$$
$$t_{n+1/2} = (n + 1/2)\Delta t, \text{ for } n \in N \text{ on the staggered mesh}$$

To preserve accuracy of the method, H is defined at $t_{n+1/2}$ on the staggered or dual time mesh and E is defined at t_n on the primary mesh. This can be visualized with time on the y-axis and space on the x-axis as per Figure 3.5.

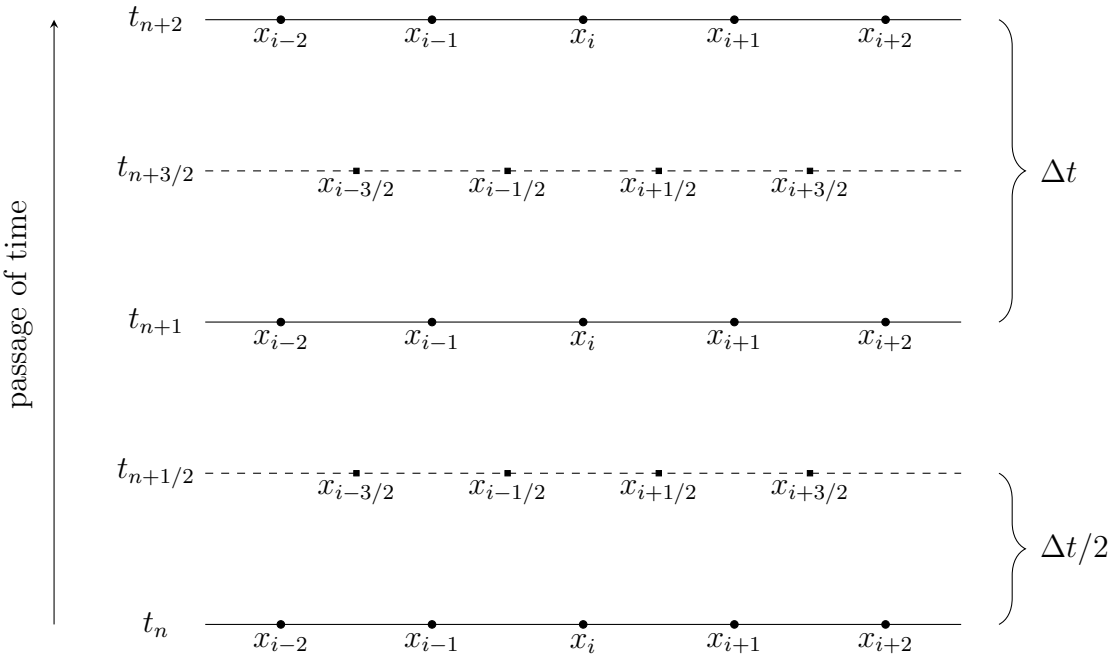

Figure 3.5: Both time and space are staggered in the 1D finite element and finite difference methods. The primary space-time mesh for the electric field is represented using dark circles, while the staggered space-time mesh for the magnetic field is represented using dark circles. This staggering in both space and time are motivated by the use of the centered finite difference.

The discrete electric field E wil lbe computed on the primary mesh in space and time, while the discrete H field will be computed on the dual or staggered mesh in space and time.

3.1.3 1D Yee Scheme

For Maxwell's Equations, we present the Yee finite difference method. Denote E_i^n as the approximation to $E(x_i, t^n)$, the exact field value. Similarly for H we denote $H_{i+1/2}^{n+1/2}$ as the approximation to the exact value $H(x_{i+1/2}^{n+1/2})$. We can then apply the finite differences to both the time (t) and space (x) derivatives in (2.9) to get

$$\begin{aligned} \varepsilon \frac{E_j^{n+1} - E_j^n}{\Delta t} &= -\frac{H_{j+1/2}^{n+1/2} - H_{j-1/2}^{n+1/2}}{\Delta x}, \\ \mu \frac{H_{j+1/2}^{n+1/2} - H_{j+1/2}^{n-1/2}}{\Delta t} &= -\frac{E_{j+1}^n - E_j^n}{\Delta x}. \end{aligned} \tag{3.4}$$

Because of the staggered nature of the meshes, these finite differences turn out to be centered differences in both space and time for the electric and magnetic fields. Multiplying (3.4) by

Δt and dividing by ε and μ respectively then gives

$$E_j^{n+1} - E_j^n = -\frac{1}{\varepsilon}\frac{\Delta t}{\Delta x}(H_{j+1/2}^{n+1/2} - H_{j-1/2}^{n+1/2}),$$
$$H_{j+1/2}^{n+1/2} - H_{j+1/2}^{n-1/2} = -\frac{1}{\mu}\frac{\Delta t}{\Delta x}(E_{j+1}^n - E_j^n).$$

Finally, the equations can be arranged such that the left hand side in the electric field equation contains terms at time $t = n + 1$ and the right side contains terms at time $t = n$ and $t = n + 1/2$. For the magnetic field, the right hand side contains terms approximating field values at $t = n$ and at $t = n - 1/2$. Thus we have

$$\begin{aligned} E_j^{n+1} &= E_j^n - \frac{1}{\varepsilon}\frac{\Delta t}{\Delta x}(H_{j+1/2}^{n+1/2} - H_{j-1/2}^{n+1/2}) \\ H_{j+1/2}^{n+1/2} &= H_{j+1/2}^{n-1/2} - \frac{1}{\mu}\frac{\Delta t}{\Delta x}(E_{j+1}^n - E_j^n) \end{aligned} \tag{3.5}$$

The left hand side now represents the value of the electric or magnetic fields at some particular points on their grid nodes *one time step in the future*. This application of finite differences is called the **Yee Scheme** and is one of the most popular finite difference methods in use. The Yee Scheme is an explicit scheme in the sense that we have explicit equations to update field values and do not have to solve a linear system at each time step. We can now model the propagation of a wave in time given some initial value at time $t = 0$.

3.1.4 Stability Conditions

For the method to produce physically meaningful solutions, certain conditions must be imposed on the relationship between Δx and Δt. As the speed of any electromagnetic wave is limited by the speed of light c_0, we must then have that the time in which the wave takes to propagate one cell, Δt, satisfies $c_0 \Delta t \leq \Delta x$ [4], [6]. Put another way, for some normalizing constant $\alpha > 0$ we have

$$\alpha c_0 \frac{\Delta t}{\Delta x} \leq 1 \quad \rightarrow \quad C_0 \Delta t = \frac{\Delta x}{\alpha} \tag{3.6}$$

If we pick a spatial step size $\Delta x > 0$, we can then put a condition on Δt that helps ensure our method correctly sticks to the physical limitations of the problems. In one spatial dimension, $\alpha = 1$ and the condition $c_0 \frac{\Delta t}{\Delta x} \leq 1$ is called a Courant Friedrich Lewy (CFL) condition. The constant α is called a Courant number. We choose $c_0 \frac{\Delta t}{\Delta x} = 1/2$ in our numerical simulation [6].

3.2 Numerical Simulations

In this section we provide several numerical simulations to demonstrate basic properties of the Yee finite difference method.

3.2.1 Periodic Boundary Conditions

This example will demonstrate the convergence of the Yee Scheme to the solution of a one-dimensional Maxwell problem with periodic boundary conditions; it will also demonstrate the effect of step size on the accuracy of the solution and show that the method is indeed second order accurate in both space and time.

For the one-dimensional set of Maxwell's Equations [for reference see Equation (2.9)], consider the exact solution to the system of partial differential equations $E(x,t) = \sin(x+t)$ and $H(x,t) = -\sin(x+t)\ \forall\ x \in \Omega$, and $t \geq 0$. Furthermore, impose periodic boundary conditions on the domain Ω where $\Omega = [0, 2\pi]$.

To simulate a numerical approximation to this exact solution, begin by discretizing Ω into two uniform meshes; the primary electric mesh τ_j and the staggered magnetic mesh $\tau_{j+1/2}$ in space. We then have the formal definitions

$$\tau_j = \{x_j \in \Omega \mid j \in 0, 1, \ldots, N;\ x_j = jh;\ x_0 = x_N\} \tag{3.7}$$

$$\tau_{j+1/2} = \{x_{j+1/2} \in \Omega \mid j \in 0, 1, \ldots, N-1;\ x_{j+1/2} = (j + 1/2)h\} \tag{3.8}$$

The number of points that the primary mesh is divided into is denoted N and is directly related to the amount of error in the numerical approximation. In order to illustrate this, the method will be used with τ_j divided into $N = 2^3, 2^4, \ldots, 2^9$ points.

We can interpret Ω as being a circular domain such that the solution is the same at the beginning point x_0 and ending point x_N. Periodic boundary conditions necessitate that both the exact and numerical solutions for the *electric* field have the same value on the "endpoints" of Ω, or that $E(0,t) = E(2\pi, t)$ for all $t > 0$.

The Yee Scheme, as given in Equation (3.5), with $\mu = \varepsilon = 1$ (i.e., $\varepsilon_0 = 1$), is then used to approximate the exact solution at time $t = 20\pi$, again with varying values of N. MATLAB code for this is given in the Appendix.

The code results in several plots, four of which are given in Figure 3.7; one for each value of N in the problem. Note that as N increases (that is, as step size decreases) the resolution of the solutions becomes higher and the approximations plotted become drastically smoother.

For cases of $N \geq 64$, the approximations and exact solutions are indistinguishable on MATLAB plots. The numerical solution appears to be closer to the exact value; this is confirmed in Figure 3.1. In the table given in Figure 3.1, the error value is obtained by performing a sum over the squared differences between the exact and numerical values; for the exact solution E_{exact}, the error in the approximation is given by the following:

$$\mathcal{E}_N(t) = \sum_{j=1}^{N} \left(\left|E_j^n - E\left(x_j, t_n\right)\right|\right)^2. \tag{3.9}$$

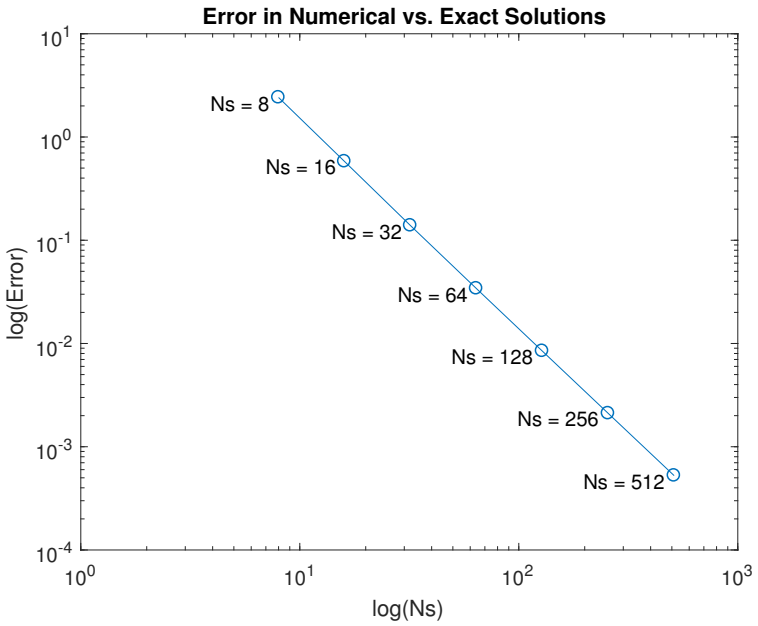

Figure 3.6: A graph of the error in the discrete electric field solution computed by the 1-D Yee Scheme. As the step size decreases by a factor of 2, the error decreases by a factor of 2^2, or 4 demonstrating that the method is second order.

N	Step Size (h)	$\mathcal{E}(20\pi)$	Error Ratio
8	0.3927	2.4144	0
16	0.19635	0.58002	4.1625
32	0.098175	0.13891	4.1755
64	0.049087	0.0304096	4.0741
128	0.024544	0.0084529	4.0336
256	0.012272	0.0021047	4.0161
512	0.0061359	0.00052514	4.0079

Table 3.1: Table of Errors for the discrete electric field in the solution computed by the 1D Yee Scheme with Periodic BC.

We define the error ratio to be

$$\frac{\mathcal{E}_N(t)}{\mathcal{E}_{2N}(t)}.$$

The value of four for the error ratio represents that a decrease in step size by a factor of two (halving the step size) leads to a decrease in error by a factor of four (quartering the error), consistent with a second-order method. Figure 3.6 shows the logarithms of the errors on a log-log plot against $\log(N)$. The line connecting them has a slope of 2, again representing that the Yee Scheme is a second order method.

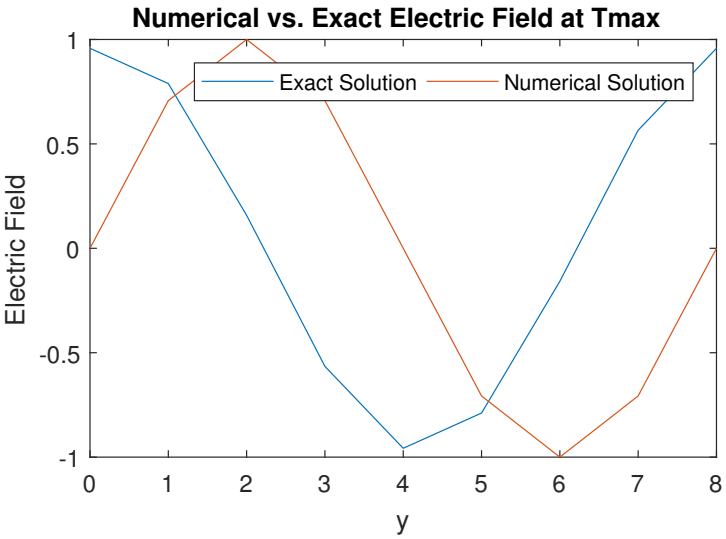

(a) $N = 8$

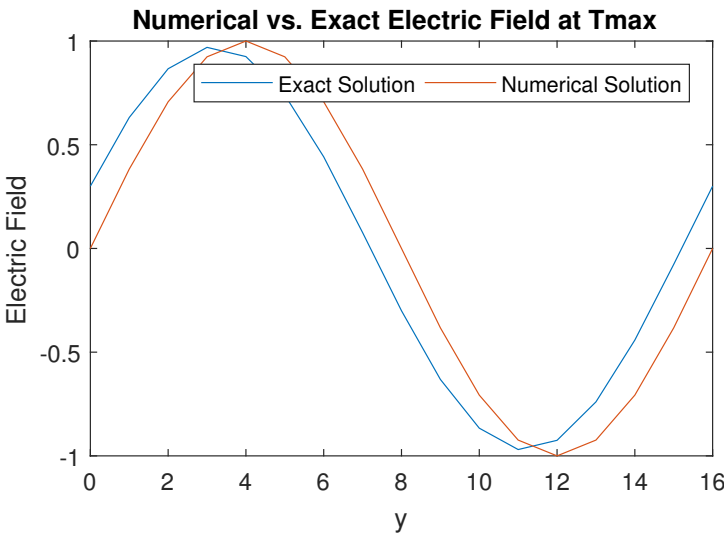

(b) $N = 16$

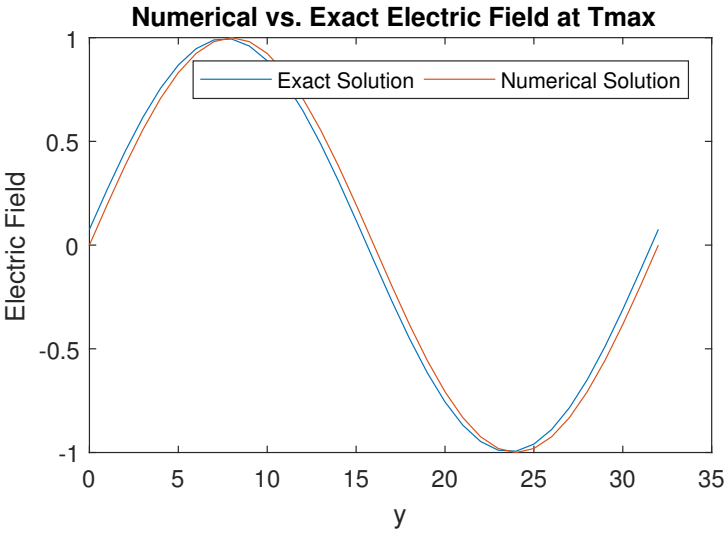

(c) $N = 32$

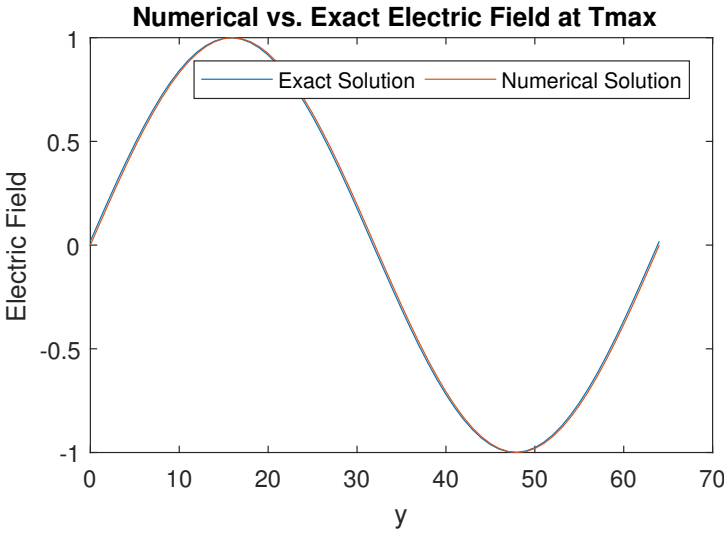

(d) $N = 64$

Figure 3.7: Numerical vs. exact solutions to the periodic boundary condition problem with several different step sizes, illustrating the reduction in error as the number of steps in the mesh increases.

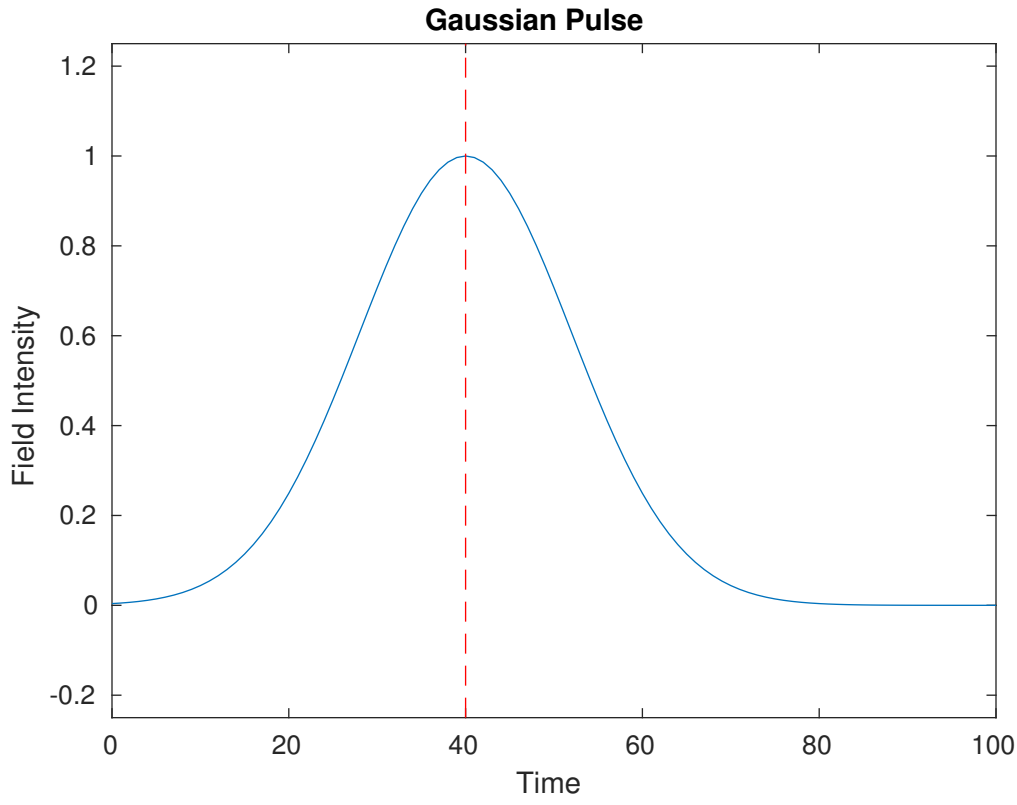

;

Figure 3.8: An example Gaussian pulse, centered at $t = 40$ and with a width of 12 units. The dotted red line, plotted at $x = 40$, lies at the center of the Gaussian pulse.

3.2.2 Gaussian Pulse Propagation

This example will demonstrate the convergence of the Yee Scheme to the solution of a one-dimensional Maxwell problem. In this example, the exact solution that the Yee Scheme models is a Gaussian pulse. The equation for a Gaussian pulse we are using is

$$f(x) = e^{-\frac{1}{2}\left(\frac{c-t}{s}\right)^2} \tag{3.10}$$

where c controls the position of the center of the peak, and s controls the width of the curve. An example is given in Figure 3.8, with the values $c = 40$ and $s = 12$. To approximate the propagation of this wave, a cell chosen at the central point (in general an arbitrary point will do) within the discretized domain Ω is set to the value of the pulse at each time step $t_n = n\Delta t$. This then allows the propagation of the pulse to be simulated through space. The boundary conditions are different here versus the Periodic Boundary Conditions example; here we assume that $E(t, x) = 0$ on the boundary. This in turn simulates a boundary that acts as a hard wall from which the pulse bounces back.

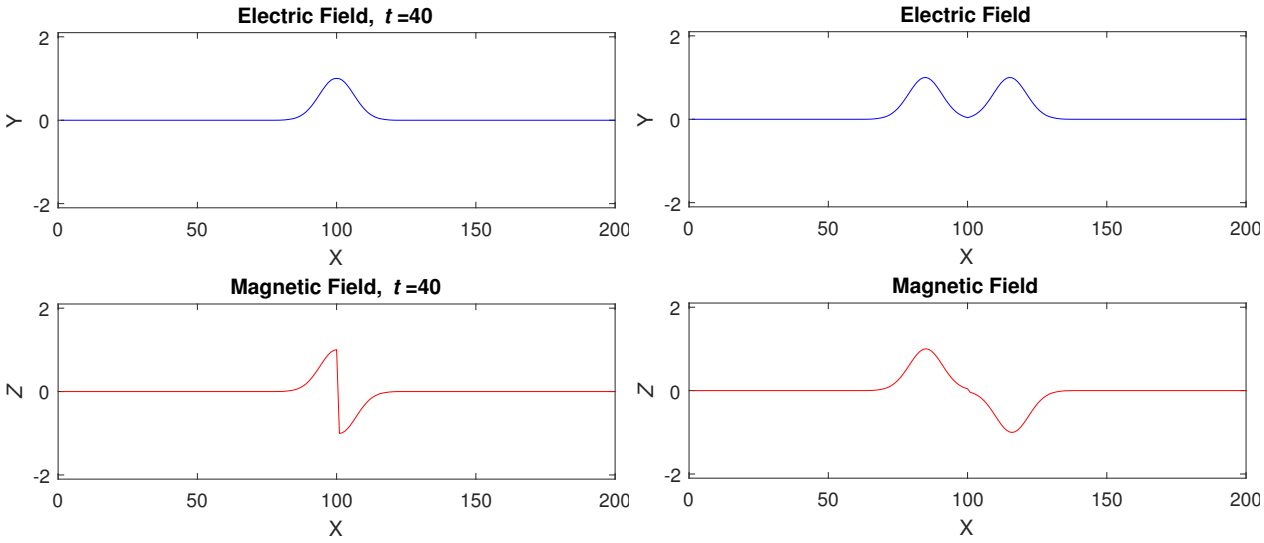

(a) $t = 40$

(b) $t = 70$

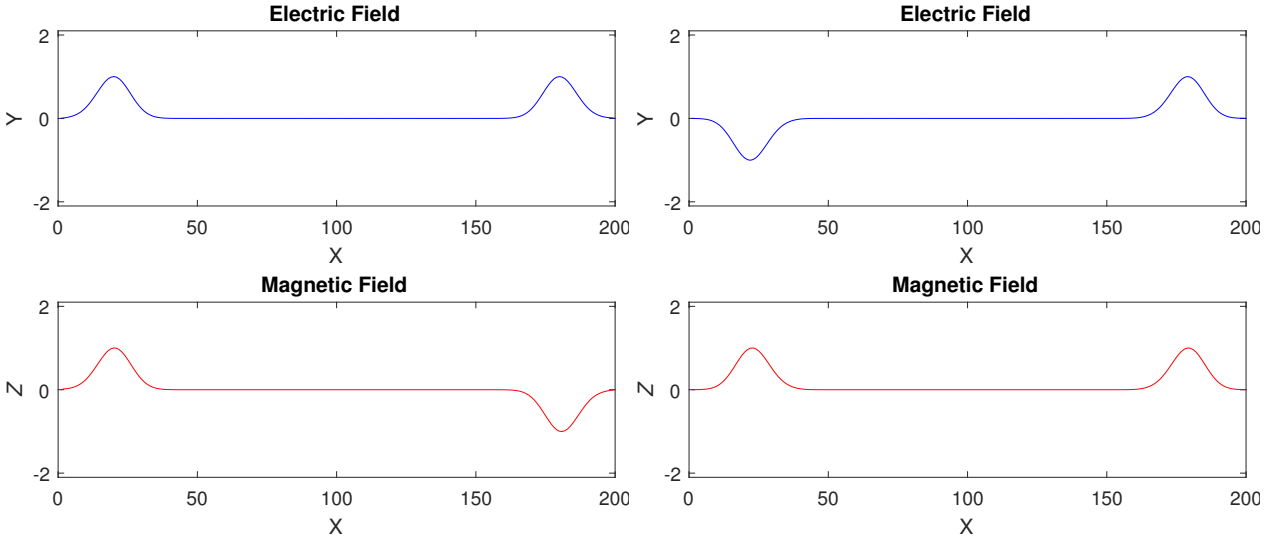

(c) $t = 200$

(d) $t = 280$

Figure 3.9: Propagation of a Gaussian Pulse at times $t = 40, 70, 200, 280$. Note the reflection from the boundary between $t = 200$ and $t = 280$.

As can be seen in Figure 3.9, the Gaussian Pulse propagates outward through space from the center as time passes. The magnetic field displays a different behavior thanks to the orthogonality inherent in Maxwell's equations; the magnetic field is negative in the "negative direction". Of particular note is the behavior of the approximation when it encounters the boundary; between $t = 200$ and $t = 280$, the pulse in both the magnetic and electric fields "bounces" off the boundary, with the left hand side of both the electric field and magnetic field flipping directions.

4 Finite Element Methods

The Finite Element Method for Maxwell's equations given as in 2.9 is based on reformulating the PDEs in integral form, called the variational formulation. To simplify notation, we denote $E_y = E$ and $H_z = H$.

4.1 Variational Formulations

To derive the variational formulation of the 1D Maxwell system (given in Equation 2.9, here rewritten so that all terms are on one side of the equation), first begin by choosing boundary conditions. We choose the Dirichlet or zero boundary condition that $E = 0$ on $\partial\Omega$, or that E is 0 on the boundary of the domain Ω, for all $t \geq 0$.

The next step is then multiplying each equation by a test function and then integrating both equations in the system across the boundary of the problem, Ω. It should also here be recalled that in the 1D system of choice, both E and H are functions of both x and t. In general the choice of test function depends on the boundary conditions of the problem. These test functions are here denoted $\psi(x)$ and $\phi(x)$. They are functions of x alone, contrasting with $E(x,t)$ and $H(x,t)$ which are functions of both space and time.

One further constraint, based on boundary conditions, lies on the functions E, H, ϕ and ψ. $H(t)$ for all $t \geq 0$ and ψ, without this constraint, can be defined to be in $L^2(\Omega)$, the Lebesgue functional space of square integrable functions on Ω. This means that they are functions for which the integral of the square of the function is finite. We will require that the functions E, ϕ and their first (weak) derivatives are in $L^2(\Omega)$.

The functions E and ϕ have an additional requirement forced by the boundary condition, namely that E and ϕ are zero on the boundary $\partial\Omega$. This requires a different space to be defined for these functions, i.e. we require $E(t)\ \forall\ t \geq 0$ and ϕ to belong to

$$H_0^1(\Omega) = \left\{ u(x) \in L^2(\Omega) \;\middle|\; \frac{du}{dx} \in L^2(\Omega), u = 0 \text{ on } \partial\Omega \right\}$$

The resulting integral form of the problem is then given to be

Find $E(t) \in H_0^1(\Omega), H(t) \in L^2(\Omega)\ \forall t > 0$ such that

$$\varepsilon \int_\Omega \frac{\partial E(t,x)}{\partial t}\phi(x)dx + \int_\Omega \frac{\partial H(t,x)}{\partial x}\phi(x)dx = 0, \tag{4.1a}$$

$$\mu \int_\Omega \frac{\partial H(t,x)}{\partial t}\psi(x)dx + \int_\Omega \frac{\partial E(t,x)}{\partial x}\psi(x)dx = 0. \tag{4.1b}$$

The next operation comes in performing integration by parts on the H term in (4.1a). As function ϕ is $\in H_0^1(\Omega)$, $\phi = 0$ on $\partial\Omega$, the operation of integration by parts then yields

$$\int_\Omega \frac{\partial H}{\partial x}\phi(x)dx = H\phi(x)\Big|_\Omega - \int_\Omega H\frac{\partial \phi(x)}{\partial x}dx = -\int_\Omega H\frac{\partial \phi(x)}{\partial x}dx$$

Substituting this into the integral forms above then gives the 1-D variational formulation that will be used for Maxwell's equations.

$$\begin{aligned} \varepsilon \int_\Omega \frac{\partial E(t,x)}{\partial t}\phi(x)dx - \int_\Omega \frac{\partial \phi(x)}{\partial x}H(t,x)dx = 0 \\ \mu \int_\Omega \frac{\partial H(t,x)}{\partial t}\psi(x)dx + \int_\Omega \frac{\partial E(t,x)}{\partial x}\psi(x)dx = 0 \end{aligned} \tag{4.2}$$

4.2 Discretization

We discretize Ω into a pair of staggered meshes as previously described and define a series of piecewise polynomial basis functions in order to obtain a problem with finite computation.

A key distinguishing feature of finite element methods is the denotation of the mesh interval $[x_p, x_{p+1}]$ as an *element*, the same abstraction that gives finite element methods their name. Each element is labeled with the index its left endpoint takes; put another way, element p denotes the segment $[x_p, x_{p+1}]$.

An issue in discretizing functions for a finite element method is that the spaces the functions are defined on are infinite-dimensional spaces. A solution to this is selecting finite dimensional subspaces of L^2 and $H_0^1(\Omega)$. Define the first of two finite-dimensional families of subspaces, denoted $V_h^1(\Omega) \subset H_0^1(\Omega)$, as

$$V_h^1(\Omega) = \left\{ u_h \in C^0(\bar{\Omega}) \mid \forall\ p = 0, 1, 2, \ldots, N-1\ u_h|_{[x_p, x_{p+1}]} \in \mathbb{P}_1, u_h(0) = u_h(1) = 0 \right\} \tag{4.3}$$

such that every element of $V_h^1(\Omega)$ is made up of a linear combination of its basis functions $u_j(x)$. This space is a discretization for the electric field E in our one-dimensional case at some time point; essentially, it is associated with E in such a way that E can be constructed from a linear combination of elements within the subspace, as can ϕ.

$V_h^1(\Omega)$ is a space of functions that are globally continuous, and piecewise linear on each of the elements $[x_p, x_{p+1}]$. The order of the space, denoted by the superscript 1 in $V_h^1(\Omega)$, is the order of the polynomials that each f takes when on an element, and the h subscript denotes that it is imposed on the discretized form of Ω. $V_h^1(\Omega)$ is also known as the Lagrange finite element space of order 1 associated to Ω. Finally, $V_h^1(\Omega)$ obeys the boundary conditions set in the problem, as it is a subspace of $H_0^1(\Omega)$.

One more finite dimensional space of functions is needed; this space is denoted $W_h^0(\Omega)$. It is similarly defined to $V_h^1(\Omega)$ with two differences; in the order of the polynomials formed and in the continuity required of its members.

$$W_h^0(\Omega) = \left\{ \mathrm{G}_h \in \mathrm{L}^2(\Omega) \;\middle|\; \forall\, p = 1, 2, \ldots, N,\ \mathrm{G}_h|_{[x_p, x_{p+1}]} \in \mathbb{P}_0 \right\} \tag{4.4}$$

As $V_h^1(\Omega)$ was associated with E and ϕ, $W_h^0(\Omega)$ is a discretized representation of H. Members of $W_h^0(\Omega)$ form, via a linear combination, H at some time point. $W_h^0(\Omega)$ does not require continuity across neighboring elements where $V_h^1(\Omega)$ does, and has polynomials of order one less than $V_h^1(\Omega)$ on each element.

Armed with these finite dimensional subspaces, there is only one step left before the definition of basis functions. Consider briefly the r-order Lagrange FEM space $V_h^r(\Omega)$; its members are piecewise-defined polynomials of degree r. For each $\mathrm{F}_h \in V_h^r(\Omega)$ to be such a polynomial, it requires $r - 1$ points in the interior of each element for its interpolation. These points are where the piecewise polynomials will be defined and are called interpolation points.

Returning to the 1D case, $V_h^1(\Omega)$ has polynomial elements of degree 1, meaning in this case 0 additional points are required in the interior of the elements. If the order of our method increased beyond one, additional interpolation points would be needed on each element.

4.3 Basis Functions

Define the function $\lambda_p(x) \in V_h^1(\Omega)$ to be the first order Lagrange basis polynomial at the point x_p. More formally, define

$$\lambda_p(x) = \begin{cases} \left(\dfrac{x - x_{p-1}}{x_p - x_{p-1}} \right), & \text{for } x \in [x_{p-1}, x_p]\,, \\ \left(\dfrac{x - x_{p+1}}{x_p - x_{p+1}} \right), & \text{for } x \in [x_p, x_{p+1}]\,, \\ 0 & \text{otherwise.} \end{cases} \tag{4.5}$$

Note λ_p has support on both $[x_{p-1}, x_p]$ and $[x_p, x_{p+1}]$. This function has the exceedingly useful property that it evaluates to 1 at the point x_p, and at every other discrete point $x_{j \neq p}$ evaluates to 0, as shown in Figure 4.1.

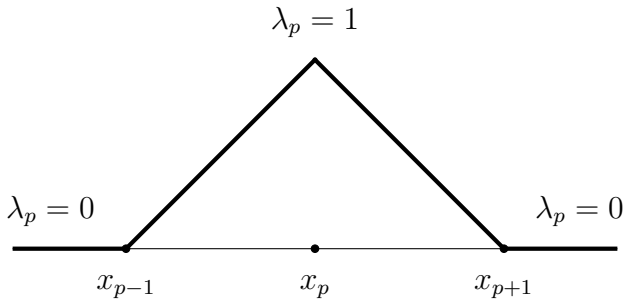

Figure 4.1: λ_p, the Lagrange polynomial basis function at x_p

A collection formed by the functions $\{\lambda_0, \lambda_1, \lambda_2, \ \dots \ , \lambda_N\}$ each associated with respective $x_0, \ \dots \ , x_N$ is a basis for $V_h^1(\Omega)$. We then call each of the λ_p basis functions. Additionally, any function in $V_h^1(\Omega)$ can be formed through a linear combination of these basis functions.

To form a basis for $W_h^0(\Omega)$, define the zeroth-degree Lagrange polynomial basis function $\lambda_{p+1/2}$ as

$$\lambda_{p+1/2} = \begin{cases} 1, & \text{for } x \in [x_p, x_{p+1}], \\ 0 & \text{otherwise.} \end{cases} \tag{4.6}$$

An example of this is given in Figure 4.2. The collection of these functions

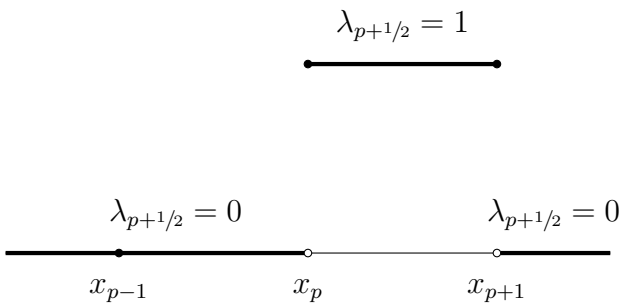

Figure 4.2: $\lambda_{p+1/2}$, the zeroth degree Lagrange polynomial basis function nonzero on $[x_p, x_{p+1}]$

$\left\{\lambda_{1/2}, \lambda_{3/2}, \ \dots \ , \lambda_{N-1/2}\right\}$ each associated with respective $x_{1/2}, \ \dots \ , x_{N-1/2}$ is a basis for $W_h^0(\Omega)$. Similarly to the collection of $\{\lambda_p\}_{x_p \in \Omega}$, any function in $W_h^0(\Omega)$ can be formed through a linear combination of these basis functions $\{\lambda_{p+1/2}\}_{x_{p+1/2}} \in \Omega$.

We have constructed these basis functions for $V_h^1(\Omega)$ and $W_h^0(\Omega)$; but what is their purpose? Briefly consider the 1D variational formulations from Equation (4.2), specifically the first expression. In the first term, a function of both x and t is derived with respect to t, and in the second term a function of x and t is derived with respect to x. With these new basis functions we have defined, we can decompose the discrete representation of $E(x,t)$ in $V_h^1(\Omega)$ denoted $E_h(x,t)$ into a linear combination, formed by products of basis functions $\lambda_p(x)$ and scalars $E_p(t)$; a keen-eyed reader may have spotted that $E_p(t)$ is a function of time, but for

now we will consider the system as a whole at a single time t leaving the discretization of time for another step.

This will result in a form that is discrete in space but continuous in time; however a time discretization can then be performed to result in a fully discrete formulation. Again note that these scalars $E_p(t)$ are actually functions of time.

Armed with this new tool we can describe $E_h(x,t) \in V_h^1(\Omega)$ by

$$E_h(x,t) = \sum_{p=0}^{N} E_p(t)\lambda_p(x). \tag{4.7}$$

This result is very important as it separates the variables t and x in the expression for $E_h(x,t)$; a similar process can be performed for $H_h(x,t)$, a discretized magnetic field. Note that as $H_h(x,t)$ is associated with the intervals between mesh points, there are $N-1$ such intervals giving

$$H_h(x,t) = \sum_{p=0}^{N-1} H_{p+1/2}(t)\lambda_{p+1/2}(x). \tag{4.8}$$

Only one more pair of terms in the continuous variational formulation must be discretized: the test functions $\psi(x)$ and $\phi(x)$. One extremely convenient choice, and one we will make, is to choose the test functions to also be linear combinations of their respective Lagrange polynomial basis functions and associated coefficients α_p and $\beta_{p+1/2}$; or that

$$\phi_h(x) = \sum_{p=0}^{N} \alpha_p \lambda_p(x); \alpha_p \in \mathbb{R}$$
$$\psi_h(x) = \sum_{p=0}^{N-1} \beta_{p+1/2} \lambda_{p+1/2}(x); \beta_{p+1/2} \in \mathbb{R}$$

The choice of the test functions to be identical to the basis functions is called Galerkin's method [4].

Substituting our basis function forms of $E_h(x,t)$, $H_h(x,t)$,$\psi_h(x)$, and $\phi_h(x)$ into the variational formulation then gives

$$\varepsilon \int_\Omega \left[\frac{\partial}{\partial t}\sum_{k=0}^{N} E_k(t)\lambda_k(x)\right]\lambda_\ell(x)\,dx$$
$$- \int_\Omega \left[\frac{\partial}{\partial x}\alpha_\ell\lambda_\ell(x)\right]\left[\sum_{k=0}^{N-1} H_{k+1/2}(t)\lambda_{k+1/2}(x)\right]dx = 0 \text{ for } \ell = 0,1,2,\ldots,N, \tag{4.9}$$

$$\mu \int_\Omega \left[\frac{\partial}{\partial t} \sum_{p=0}^{N-1} H_{p+1/2}(t) \lambda_{p+1/2}(x) \right] \lambda_{j+1/2}(x)\, dx$$
$$+ \int_\Omega \left[\frac{\partial}{\partial x} \sum_{p=0}^{N} E_p(t) \lambda_p(x) \right] \lambda_{j+1/2}(x)\, dx = 0 \text{ for } j = 0, 1, 2, \ldots, N-1. \quad (4.10)$$

4.4 Matrix Assembly

Define the row vector $\vec{E}_h(t)$ to be the collection, in order, of all E_p terms in the discretization of $E(x,t)$:

$$\vec{E}_h(t) = [E_0(t), E_1(t), \ldots, E_N(t)]^T$$

The row vector $\vec{H}_h(t)$ is a similarly defined collection of all H_p terms:

$$\vec{H}_h(t) = \left[H_{1/2}(t), H_{3/2}(t), \ldots, H_{(N\,-\,1/2)/2}(t)\right]^T$$

By the definition of $\lambda_j(x)$, we have for $|j-k| \geq 2, \lambda_j(x)\lambda_k(x) = 0$ as on any interval where $\lambda_j(x)$ is nonzero, $\lambda_k(x)$ is zero. Then we define the electric mass matrix

$$M_E = \begin{bmatrix} \int_\Omega \lambda_0\lambda_0 dx & \int_\Omega \lambda_1\lambda_0 dx & 0 & & \ldots & 0 \\ \int_\Omega \lambda_0\lambda_1 dx & \int_\Omega \lambda_1\lambda_1 dx & \int_\Omega \lambda_2\lambda_1 dx & & \ldots & 0 \\ 0 & \int_\Omega \lambda_1\lambda_2 dx & \int_\Omega \lambda_2\lambda_2 dx & & \ldots & 0 \\ \vdots & \vdots & \vdots & \ddots & \int_\Omega \lambda_{N_r-2}\lambda_{N_r-2} dx & \int_\Omega \lambda_{N_r-1}\lambda_{N_r-2} dx \\ 0 & 0 & 0 & \ldots & \int_\Omega \lambda_{N_r-2}\lambda_{N_r-1} dx & \int_\Omega \lambda_{N_r-1}\lambda_{N_r-1} dx \end{bmatrix}$$

The diagonal of this matrix follows a certain pattern. The mass matrix on elements $p-1$ and p is given by

$$M_E^{\text{local}} = \begin{bmatrix} \int_\Omega \lambda_{x_{p-1}}\lambda_{x_{p-1}} dx & \int_\Omega \lambda_{x_p}\lambda_{x_{p-1}} dx & 0 \\ \int_\Omega \lambda_{x_{p-1}}\lambda_{x_p} dx & \int_\Omega \lambda_{x_p}\lambda_{x_p} dx & \int_\Omega \lambda_{x_{p+1}}\lambda_{x_p} dx \\ 0 & \int_\Omega \lambda_{x_p}\lambda_{x_{p+1}} dx & \int_\Omega \lambda_{x_{p+1}}\lambda_{x_{p+1}} dx \end{bmatrix}$$

Computing the first integral $\int\limits_{\Omega} \lambda_p(x)\lambda_{p-1}(x)dx$:

$$\int\limits_{\Omega} \lambda_p(x)\lambda_{p-1}(x)dx = \int\limits_{x_{p-1}}^{x_p} \lambda_p(x)\lambda_{p-1}(x)dx =$$

$$-\frac{1}{h^2}\int\limits_{x_{p-1}}^{x_p} (x - x_{p-1})\,(x - x_p)\,dx = -\frac{1}{h^2}\left(\frac{x^3}{3} - \frac{x_p x^2}{2} - \frac{x_{p-1}x^2}{2} + x_{p-1}x_p x\Big|_{x_{p-1}}^{x_p}\right) =$$

$$-\frac{1}{6h^2}\left(2(x_p^3 - x_{p-1}^3) - 3x_p(x_p^2 - x_{p-1}^2) - 3x_{p-1}(x_p^2 - x_{p-1}^2) + 6x_p x_{p-1}(x_p - x_{p-1})\right) =$$

$$-\frac{1}{6h^2}\,(x_{p-1} - x_p)^3 = -\frac{1}{6h^2}\,(-h)^3 = h\frac{1}{6}$$

The second integral integral $\int\limits_{\Omega} \lambda_p(x)^2 dx$ can be attacked by splitting into two integrals:

$$\int\limits_{\Omega} \lambda_p(x)^2 dx = \overbrace{\frac{1}{h^2}\int\limits_{x_p-1}^{x_p} (x - x_{p-1})^2 dx}^{①} + \overbrace{\frac{1}{h^2}\int\limits_{x_p}^{x_p+1} (x - x_{p+1})^2 dx}^{②} \to$$

$$① : \frac{1}{h^2}\int\limits_{x_p-1}^{x_p} (x - x_{p-1})^2 dx = \frac{1}{h^2}\int\limits_{0}^{x_p - x_{p-1}} u^2 du \quad \text{[with } u \text{ substitution } u = x - x_{p-1},\ du = dx\text{]}$$

$$= \frac{1}{3h^2}\left(u^3\Big|_0^h\right) = h\frac{1}{3} \to$$

$$② : \frac{1}{h^2}\int\limits_{x_p}^{x_p+1} (x - x_{p+1})^2 dx = \frac{1}{h^2}\int\limits_{x_p - x_{p+1}}^{0} u^2 dx \quad \text{[with } u \text{ substitution } u = x - x_{p+1},\ du = dx\text{]}$$

$$= \frac{1}{3h^2}\left(u^3\Big|_{-h}^0\right) = h\frac{1}{3} \to ① + ② = h\frac{2}{3}$$

And the third integral

$$\int_{\Omega} \lambda_p(x)\lambda_{p+1}(x)dx = \int_{x_p}^{x_{p+1}} \lambda_p(x)\lambda_{p+1}(x)dx$$

$$= -\frac{1}{h^2}\int_{x_p}^{x_{p+1}} (x-x_p)\,(x-x_{p+1})\,dx = -\frac{1}{h^2}\left(\frac{x^3}{3} - \frac{x_{p+1}x^2}{2} - \frac{x_p x^2}{2} + x_p x_{p+1} x\Big|_{x_p}^{x_{p+1}}\right) =$$

$$-\frac{1}{6h^2}\,(x_p - x_{p+1})^3 = h\frac{1}{6}$$

This is true for any elements on the diagonal of M_E. Then M_E can be written as

$$M_E^{\text{local}} = h\begin{bmatrix} 2/3 & 1/6 & 0 \\ 1/6 & 2/3 & 1/6 \\ 0 & 1/6 & 2/3 \end{bmatrix}$$

Note that the far upper left and lower right entries of the matrix, those corresponding to $\int_{x_0}^{x_1} \lambda_{x_0}(x)^2 dx$ and $\int_{x_{N_r-2}}^{x_{N_r-1}} \lambda_{x_{N_r-1}}(x)^2 dx$, may have different values as the regions of support for the basis functions are defined by the boundary conditions of the problem. The staggered basis function $\lambda_{x_{p+1/2}}$ is defined on $[x_p, x_{p+1}]$; we define the Stiffness matrix

$$S = \begin{bmatrix} \int_\Omega \lambda_{1/2}\frac{\partial}{\partial x}\lambda_0 dx & 0 & 0 & & \dots & 0 \\ \int_\Omega \lambda_{1/2}\frac{\partial}{\partial x}\lambda_1 dx & \int_\Omega \lambda_{\frac{3}{2}}\frac{\partial}{\partial x}\lambda_1 dx & 0 & & \dots & 0 \\ 0 & \int_\Omega \lambda_{\frac{3}{2}}\frac{\partial}{\partial x}\lambda_2 dx & \int_\Omega \lambda_{\frac{5}{2}}\frac{\partial}{\partial x}\lambda_2 dx & & \dots & 0 \\ \vdots & \vdots & \vdots & \ddots & & \vdots \\ & & & & \int_\Omega \lambda_{N_r-\frac{3}{2}}\frac{\partial}{\partial x}\lambda_{N_r-2} dx & 0 \\ 0 & 0 & 0 & \dots & \int_\Omega \lambda_{N_r-\frac{3}{2}}\frac{\partial}{\partial x}\lambda_{N_r-1} dx & \int_\Omega \lambda_{N_r-\frac{1}{2}}\frac{\partial}{\partial x}\lambda_{N_r-1} dx \end{bmatrix}$$

This lower bidiagonal matrix on elements $p-1$ and p is given by

$$S^{\text{local}} = \begin{bmatrix} \int_\Omega \lambda_{p-\frac{1}{2}}\frac{\partial}{\partial x}\lambda_{p-1} dx & 0 & 0 \\ \int_\Omega \lambda_{p-\frac{1}{2}}\frac{\partial}{\partial x}\lambda_p dx & \int_\Omega \lambda_{p+\frac{1}{2}}\frac{\partial}{\partial x}\lambda_p dx & 0 \\ 0 & \int_\Omega \lambda_{p+\frac{1}{2}}\frac{\partial}{\partial x}\lambda_{p+1} dx & \int_\Omega \lambda_{p+\frac{3}{2}}\frac{\partial}{\partial x}\lambda_{p+1} dx \end{bmatrix}$$

Solving the first integral $\int\limits_{\Omega} \lambda_{p-\frac{1}{2}} \frac{\partial}{\partial x} \lambda_{p-1} dx$:

$$\int\limits_{\Omega} \lambda_{p-\frac{1}{2}} \frac{\partial}{\partial x} \lambda_{p-1} dx = \int\limits_{x_{p-1}}^{x_p} \lambda_{p-\frac{1}{2}} \frac{\partial}{\partial x} \lambda_{p-1} dx = \int\limits_{x_{p-1}}^{x_p} (1) \frac{\partial}{\partial x} \left(\frac{1}{-h} (x - x_{p-1}) \right) dx$$
$$= -\frac{1}{h} \int\limits_{x_{p-1}}^{x_p} 1 \, dx = -\frac{1}{h} \left(x \Big|_{x_{p-1}}^{x_p} \right) = -1$$

And the second integral $\int\limits_{\Omega} \lambda_{p-\frac{1}{2}} \frac{\partial}{\partial x} \lambda_{p} dx$:

$$\int\limits_{\Omega} \lambda_{p-\frac{1}{2}} \frac{\partial}{\partial x} \lambda_{p} dx = \int\limits_{x_{p-1}}^{x_p} \lambda_{p-\frac{1}{2}} \frac{\partial}{\partial x} \lambda_{p} dx = \int\limits_{x_{p-1}}^{x_p} (1) \frac{\partial}{\partial x} \left(\frac{1}{h} (x - x_{p}) \right) dx$$
$$= \frac{1}{h} \int\limits_{x_{p-1}}^{x_p} 1 \, dx = \frac{1}{h} \left(x \Big|_{x_{p-1}}^{x_p} \right) = 1$$

The arbitrary diagonal portion is then

$$S^{\text{local}} = \begin{bmatrix} -1 & 0 & 0 \\ 1 & -1 & 0 \\ 0 & 1 & -1 \end{bmatrix},$$

which gives the full matrix

$$S = \begin{bmatrix} -1 & 0 & 0 & & \dots & 0 \\ 1 & -1 & 0 & & \dots & 0 \\ 0 & 1 & -1 & & \dots & 0 \\ \vdots & \vdots & \vdots & \ddots & & \vdots \\ & & & & -1 & 0 \\ 0 & 0 & 0 & \dots & 1 & -1 \end{bmatrix}$$

Finally, we define the magnetic mass matrix

$$M_H = \begin{bmatrix} \int\limits_{\Omega} \lambda_{\frac{1}{2}} \lambda_{\frac{1}{2}} dx & 0 & 0 & & \dots & 0 \\ 0 & \int\limits_{\Omega} \lambda_{\frac{3}{2}} \lambda_{\frac{3}{2}} dx & 0 & & \dots & 0 \\ 0 & 0 & \int\limits_{\Omega} \lambda_{\frac{5}{2}} \lambda_{\frac{5}{2}} dx & & \dots & 0 \\ \vdots & \vdots & \vdots & \ddots & & \vdots \\ & & & & \int\limits_{\Omega} \lambda_{N_r - \frac{3}{2}} \lambda_{N_r - \frac{3}{2}} dx & 0 \\ 0 & 0 & 0 & \dots & 0 & \int\limits_{\Omega} \lambda_{N_r - \frac{1}{2}} \lambda_{N_r - \frac{1}{2}} dx \end{bmatrix}$$

The local matrix on elements $p-1$ and p is given, again by the regions of support for $\lambda_{p+\frac{1}{2}}$ and the addition property of integrals,

$$M_H^{\text{local}} = \begin{bmatrix} \int\limits_\Omega \lambda_{p-\frac{1}{2}}\lambda_{p-\frac{1}{2}}dx & 0 & 0 \\ 0 & \int\limits_\Omega \lambda_{p+\frac{1}{2}}\lambda_{p+\frac{1}{2}}dx & 0 \\ 0 & 0 & \int\limits_\Omega \lambda_{p+\frac{3}{2}}\lambda_{p+\frac{3}{2}}dx \end{bmatrix}$$

The integral $\int\limits_\Omega \lambda_{p-\frac{1}{2}}\lambda_{p-\frac{1}{2}}dx$ is

$$\int\limits_\Omega \left(\lambda_{p-\frac{1}{2}}\right)^2 dx = \int\limits_{x_{p-1}}^{x_p} \left(\lambda_{p-\frac{1}{2}}\right)^2 dx = \int\limits_{x_{p-1}}^{x_p} (1)^2\, dx = \left(x\Big|_{x_{p-1}}^{x_p} \right) dx = h$$

Which results in M_H equal to h times the identity matrix,

$$M_H = \begin{bmatrix} 1 & 0 & 0 & \dots & 0 \\ 0 & 1 & 0 & \dots & 0 \\ 0 & 0 & 1 & \dots & 0 \\ \vdots & \vdots & \vdots & \ddots & \vdots \\ 0 & 0 & 0 & \dots & 1 \end{bmatrix}$$

Thus, our discrete variational formulation can be written in matrix form as the system

$$\begin{aligned} \frac{d}{dt} M_E \vec{E}_h(t) - \vec{H}_h(t) S = 0, \\ \frac{d}{dt} M_H \vec{H}_h(t) + \vec{E}_h(t) S^T = 0. \end{aligned} \tag{4.11}$$

4.5 Time Discretization

With this semi-discrete matrix formulation, we now must now find a way to discretize this system in time. In a similar fashion to the finite difference method, the leapfrog time discretization is applied, again staggered in time for the magnetic field:

$$\begin{aligned} M_E \frac{\vec{E}_h^{n+1} - \vec{E}_h^n}{\Delta t} - S\vec{H}_h^{n+1/2} = 0 \\ M_H \frac{\vec{H}_h^{n+1/2} - \vec{H}_h^{n-1/2}}{\Delta t} + S_T \vec{E}_h^n = 0 \end{aligned} \tag{4.12}$$

The final step in obtaining the FEM is rearranging Equation (4.12) to form a truly iterative method. A caveat lies in the traditional separation of h from M_H and M_E.

$$\begin{aligned} M_E \vec{E}_h^{n+1} &= M_E \vec{E}_h^n + S\frac{\Delta t}{h}\vec{H}_h^{n+1/2} \\ M_H \vec{H}_h^{n+1/2} &= M_H \vec{H}_h^{n-1/2} - S^T\frac{\Delta t}{h}\vec{E}_h^n \end{aligned} \tag{4.13}$$

This gives exactly the FEM.

4.6 Stability Conditions

The stability conditions for the FEM given here are similar to those of the finite difference method; for the purposes of this paper, $\Delta t = h$ and $\Delta t = 0.25 * h$ are used for the periodic 1D FEM and the Lorentz metamaterial model, respectively.

4.7 Numerical Simulations

We repeat the numerical experiment performed in Section 3.2 with an exact solution satisfying periodic boundary conditions. We repeat the experiment here with the FEM instead of the Yee scheme. in Figure 43. we plot the exact and approximate electric and magnetic fields together, with $N = 4, 8, 16, 32$ and therefore $h = 1/4, 1/8, 1/16, 1/32$. Note that the problem is non-dimensionalized to set to set the amplitude of the wave to 1 so that the domain of the problem is $[0, 1]$. The solution is convergent, as we have that N increasing, and therefore h decreasing, by a factor of two doubles the accuracy of the method. We can state this as in this problem a method called mass-lumping was performed, in which the tridiagonal mass matrix M_E was transformed so that the linear system given in (4.13) is exactly the Yee scheme, which then has the convergence and order of accuracy behaviors as shown in Section 3.2. A plot of the exact vs. approximate electric and magnetic fields with this method can be found in Figure 4.3.

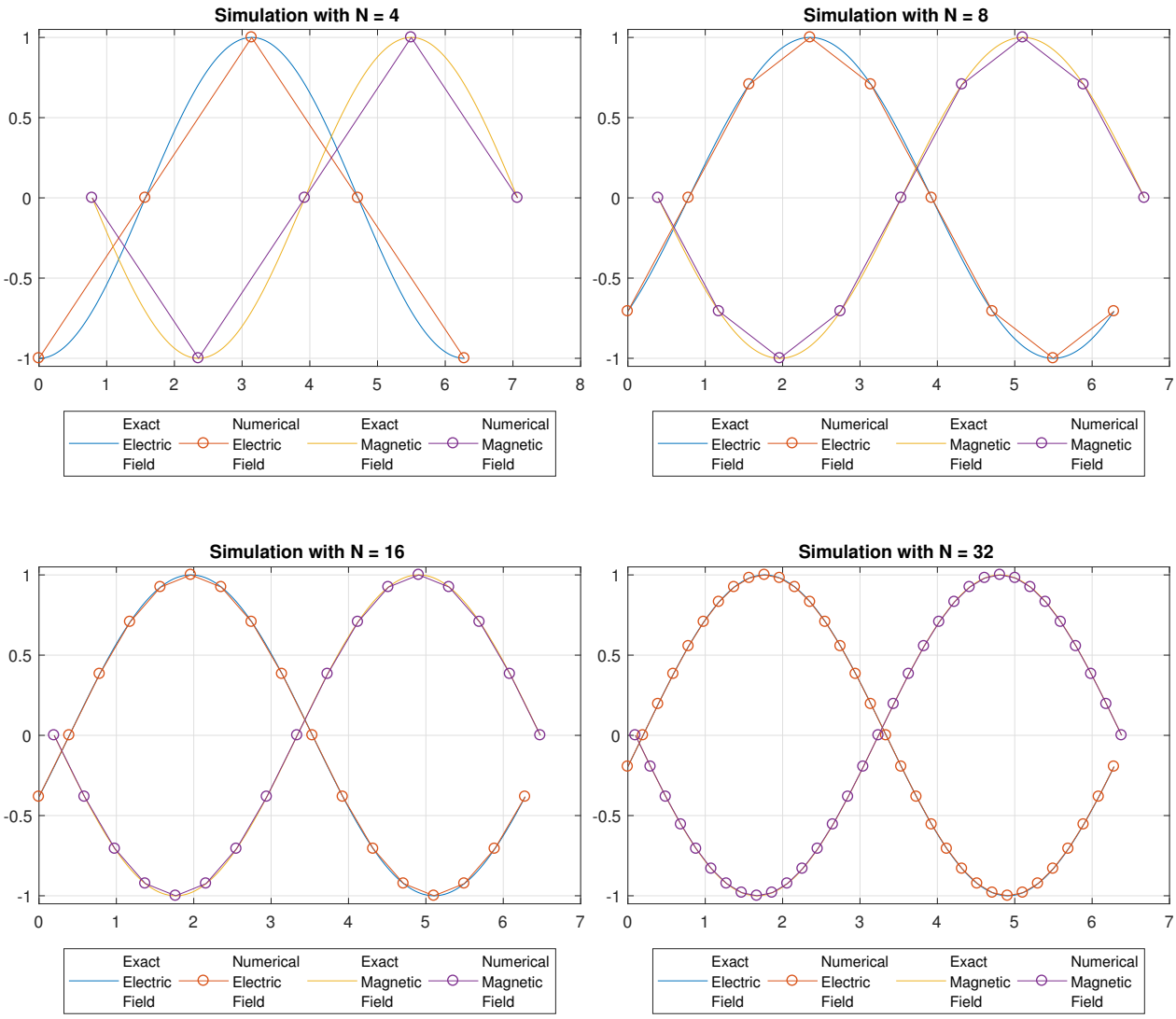

Figure 4.3: The exact and numerical solutions formed by the FEM approximation to $E(t,x) = \sin(x+t)$, $H(t,x) = -\sin(x+t)$ with 4, 8, 16 and 32 steps in the domain and periodic boundary conditions. As the number of steps increases, so does the accuracy of the method by an order of two.

5 Maxwell's Equations in Linear Metamaterials

Metamaterials are the direct result of the work of a Russian scientist named Victor Veselago, who in 1967 published a paper which described the first metamaterial; though he called them Left-Handed Materials after a physics concept behind their design, they came to have the name we are familiar with today.

Metamaterials are structured on the molecular level such that their values for permittivity and permeability are negative. Essentially, this gives the materials properties with respect to wave propagation that are not found in nature [2].

These qualities have many uses which can be divided into two broad categories; those exhibiting properties in optics and those exhibiting properties in electromagnetics outside of optics. The basic optical properties from the metamaterials in question often are distinguished by their unusual refractive index, defined as

$$n = \frac{c}{v},$$

where c is the speed of light in a vacuum and v is the velocity of the light in the material in question. For normal media, this number n is usually greater than 1 [2], but in metamaterials this is not the case.

Presented here are two models for metamaterials: the Drude and Lorentz metamaterial models. Both modify the essential Maxwell's Equations given in (2.1); the Drude model adds a term for induced currents to the Gauss-Ampére Law and Faraday's Law. The Lorentz model is similar to the Drude in that it adds induced currents, but also accounts for dissipation (decay of the wave).

Both models involve the phenomenon of physical dispersion: the permittivity and permeability in the frequency domain is a function of the angular frequency. In such materials, the speed of propagation of electromagnetic waves depends on the frequency of the wave and not constant.

5.1 Drude Metamaterial Model

The Drude Model modifies the Gauss-Ampére Law and Faraday's Law, both given in Table 2.5, to be the following:

$$\begin{aligned} \mu\frac{\partial \vec{H}}{\partial t} &= -\nabla \times \vec{E} - \vec{K} \\ \varepsilon\frac{\partial \vec{E}}{\partial t} &= \nabla \times \vec{H} - \vec{J} \end{aligned} \tag{5.1}$$

Where $\vec{K}$ and $\vec{J}$ model induced electric and magnetic currents. These are artifacts of a given metamaterial in the context of a problem. This system can be reduced to 1D by setting $\partial/\partial y = 0$ and $\partial/\partial z = 0$ and only retaining certain field components as detailed in Section 2. The decoupled systems are:

$$\begin{aligned} \varepsilon \frac{\partial E_y}{\partial t} &= -\frac{\partial H_z}{\partial x} - J_y \\ \mu \frac{\partial H_z}{\partial t} &= -\frac{\partial E_y}{\partial x} - K_z \end{aligned} \tag{5.2}$$

One further piece is needed to fully account for the behavior of a Drude Metamaterial: the constitutive laws describing the evolution in time of J and K, omitting the coordinate subscripts.

$$\frac{\partial J}{\partial t} + \Gamma_e J = \epsilon_0 \omega_{pe}^2 E, \tag{5.3}$$

or

$$\frac{1}{\epsilon_0 \omega_{pe}^2} \frac{\partial J}{\partial t} + \frac{\Gamma_e}{\epsilon_0 \omega_{pe}^2} J = E; \tag{5.4}$$

and

$$\frac{\partial K}{\partial t} + \Gamma_m K = \mu_0 \omega_{pm}^2 H, \tag{5.5}$$

or

$$\frac{1}{\mu_0 \omega_{pm}^2} \frac{\partial K}{\partial t} + \frac{\Gamma_m}{\mu_0 \omega_{pm}^2} K = H. \tag{5.6}$$

With the following parameters:

Γ_e	Electric damping frequency	ω_{e0}	Electric resonance frequency
Γ_m	Magnetic damping frequency	ω_{m0}	Magnetic resonance frequency
μ_0	Initial permeability	ω_{pe}	Electric plasma frequency
ϵ_0	Initial permittivity	ω_{pm}	Magnetic plasma frequency

Table 5.1: The values of material constants in the Drude (and Lorentz) metamaterial models.

Therefore the full system for the Drude Metamaterial then is

$$\varepsilon \frac{\partial E}{\partial t} = -\frac{\partial H}{\partial x} - J, \tag{5.7}$$

$$\mu \frac{\partial H}{\partial t} = -\frac{\partial E}{\partial x} - K, \tag{5.8}$$

$$\frac{1}{\epsilon_0 \omega_{pe}^2} \frac{\partial J}{\partial t} + \frac{\Gamma_e}{\epsilon_0 \omega_{pe}^2} J = E, \tag{5.9}$$

$$\frac{1}{\mu_0 \omega_{pm}^2} \frac{\partial K}{\partial t} + \frac{\Gamma_m}{\mu_0 \omega_{pm}^2} K = H. \tag{5.10}$$

In a similar fashion to the model for linear dielectrics, the variational formulations of (5.7) - (5.10) is given as

Find $E \in H_0^1(\Omega), H, J, K \in L^2(\Omega)$ such that

$$\varepsilon \frac{d}{dt} \int_\Omega E(x,t)\phi(x)\, dx - \int_\Omega \frac{\partial \phi(x)}{\partial t} H(x,t)\, dx + \int_\Omega J(x,t)\phi(x)\, dx = 0, \tag{5.11}$$

$$\mu \frac{d}{dt} \int_\Omega H(x,t)\psi(x)\, dx + \int_\Omega \frac{\partial E(x,t)}{\partial x} \psi(x)\, dx + \int_\Omega K(x,t)\psi(x)\, dx = 0, \tag{5.12}$$

$$\frac{1}{\epsilon_0 \omega_{pe}^2} \frac{d}{dt} \int_\Omega J(x,t)\eta(x)\, dx + \frac{\Gamma_e}{\epsilon_0 \omega_{pe}^2} \int_\Omega J(x,t)\eta(x)\, dx = \int_\Omega E(x,t)\eta(x)\, dx, \tag{5.13}$$

$$\frac{1}{\mu_0 \omega_{pm}^2} \frac{d}{dt} \int_\Omega K(x,t)\alpha(x)\, dx + \frac{\Gamma_m}{\mu_0 \omega_{pm}^2} \int_\Omega K(x,t)\alpha(x)\, dx = \int_\Omega H(x,t)\alpha(x)\, dx. \tag{5.14}$$

$\forall \phi(x) \in H_0^1(\Omega), \psi(x), \eta(x), \alpha(x) \in L^2(\Omega)$. In our discrete variational problem we choose E_h and J_h to be in $\mathcal{V}_h^1(\Omega)$ and H_h and K_h to be in $W_0^1(\Omega)$, then perform the discretization as discussed in the finite difference method.

$$\varepsilon \frac{d}{dt} M_E \vec{E}_h(x,t) - S\vec{H}_h(x,t) + M_E \vec{J}_h(x,t) = 0, \tag{5.15}$$

$$\mu \frac{d}{dt} M_H \vec{H}_h(x,t) + S^T \vec{E}_h(x,t) + M_H \vec{K}_h(x,t) = 0, \tag{5.16}$$

$$\frac{1}{\epsilon_0 \omega_{pe}^2} \frac{d}{dt} M_E \vec{J}_h(x,t) + \frac{\Gamma_e}{\epsilon_0 \omega_{pe}^2} M_E \vec{J}_h(x,t) = M_E \vec{E}_h(x,t), \tag{5.17}$$

$$\frac{1}{\mu_0 \omega_{pm}^2} \frac{d}{dt} M_H \vec{K}_h(x,t) + \frac{\Gamma_m}{\mu_0 \omega_{pm}^2} M_H \vec{K}_h(x,t) = M_H \vec{H}_h(x,t). \tag{5.18}$$

The Leapfrog time discretization can then be performed in the Gauss-Ampére Law and Faraday's Law; however in the permittivity equations, the lower order term is averaged to

give

$$\varepsilon M_E \left(\frac{\vec{E}_h^{n+1} - \vec{E}_h^n}{\Delta t} \right) - S\vec{H}_h^{n+1/2} + M_E \vec{J}_h^{n+1/2} = 0 \tag{5.19}$$

$$\mu M_H \left(\frac{\vec{H}_h^{n+1/2} - \vec{H}_h^{n-1/2}}{\Delta t} \right) + S^T \vec{E}_h^n + M_H \vec{K}_h^n = 0 \tag{5.20}$$

$$\frac{1}{\epsilon_0 \omega_{pe}^2} M_E \left(\frac{\vec{J}_h^{n+1/2} - \vec{J}_h^{n-1/2}}{\Delta t} \right) + \frac{\Gamma_e}{\epsilon_0 \omega_{pe}^2} M_E \left(\frac{\vec{J}_h^{n+1/2} + \vec{J}_h^{n-1/2}}{2} \right) = M_E \vec{E}_h^n \tag{5.21}$$

$$\frac{1}{\mu_0 \omega_{pm}^2} M_H \left(\frac{\vec{K}_h^{n+1} - \vec{K}_h^n}{\Delta t} \right) + \frac{\Gamma_m}{\mu_0 \omega_{pm}^2} M_H \left(\frac{\vec{K}_h^{n+1} + \vec{K}_h^n}{2} \right) = M_H \vec{H}_h^{n+1/2} \tag{5.22}$$

This is done in a process very similar tot he construction of the finite element method in liner dielectrics. Finally, multiplying each of the systems by the inverse of the appropriate mass matrix allows the system to be simplified, and aids the rewriting as an iterative method:

$$\vec{E}_h^{n+1} = \vec{E}_h^n + \frac{\Delta t}{\varepsilon} \left(M_E^{-1} S \vec{H}_h^{n+1/2} - \vec{J}_h^{n+1/2} \right) \tag{5.23}$$

$$\vec{H}_h^{n+1/2} = \vec{H}_h^{n-1/2} - \frac{\Delta t}{\mu} \left(M_H^{-1} S^T \vec{E}_h^n + \vec{K}_h^n \right) \tag{5.24}$$

$$\vec{J}_h^{n+1/2} = \vec{J}_h^{n-1/2} \left(\frac{2\Delta t^{-1} - \Gamma_e}{2\Delta t^{-1} + \Gamma_e} \right) + \vec{E}_h^n \left(\frac{2\epsilon_0 \omega_{pe}^2}{2\Delta t^{-1} + \Gamma_e} \right) \tag{5.25}$$

$$\vec{K}_h^{n+1} = \vec{K}_h^n \left(\frac{2\Delta t^{-1} - \Gamma_m}{2\Delta t^{-1} + \Gamma_m} \right) + \vec{H}_h^{n+1/2} \left(\frac{2\mu_0 \omega_{pm}^2}{2\Delta t^{-1} + \Gamma_m} \right) \tag{5.26}$$

5.2 Lorentz Metamaterial Model

The Lorentz model is very similar to the Drude model, but includes dissipation. It does so by adding an additional dissipative term to the constitutive laws [1]. We begin with a pair of decoupled systems similar to those given in (5.2), with the important addition of Polarization ($\vec{P}$) and Magnetization ($\vec{M}$) terms:

$$\begin{aligned} \varepsilon_0 \frac{\partial \vec{E}}{\partial t} + \vec{J} &= -\frac{\partial \vec{H}}{\partial x}, & \mu_0 \frac{\partial \vec{H}}{\partial t} + \vec{K} &= \frac{\partial \vec{E}}{\partial x}, \\ \frac{\partial \vec{P}}{\partial t} &= \vec{J}, & \frac{\partial \vec{M}}{\partial t} &= \vec{K}, \\ \frac{\partial \vec{J}}{\partial t} + \Gamma_e \vec{J} + \omega_{e0}^2 \vec{P} &= \varepsilon_0 \omega_{pe}^2 \vec{E}, & \frac{\partial \vec{K}}{\partial t} + \Gamma_m K + \omega_{m0}^2 \vec{M} &= \mu_0 \omega_{pm}^2 \vec{H}. \end{aligned} \tag{5.27}$$

How are these obtained? Firstly, in any material the polarization $\vec{P}$ (related to the electric field) and magnetization $\vec{M}$ (related to the magnetic field) are defined in the frequency

domain as

$$\hat{\vec{P}} = \varepsilon_0 \chi_e \hat{\vec{E}},$$
$$\hat{\vec{M}} = \mu_0 \chi_m \hat{\vec{H}},$$

with χ_e and χ_m the electric and magnetic susceptibilities, both properties of the metamaterial, and ε_0 and μ_0 the free-space permittivity and permeability and the $\hat{}$ denotes a Fourier transform. What are the values of $\chi_e(\omega)$ and $\chi_m(\omega)$? In the Lorentz case the susceptibilities are given to be functions of angular frequency ω as

$$\chi_e = \frac{\omega_{pe}^2}{\omega_{e0}^2 - \omega^2 + i\Gamma_e \omega},$$
$$\chi_m = \frac{\omega_{pm}^2}{\omega_{m0}^2 - \omega^2 + i\Gamma_m \omega},$$

where the constants ω_{e0}, Γ_m, etc. are the same as those discussed in the Drude model (Table 5.1) and i the imaginary constant with $i^2 = -1$. Then we have that

$$\hat{\vec{P}} = \varepsilon_0 \frac{\omega_{pe}^2}{\omega_{e0}^2 - \omega^2 + i\Gamma_e \omega} \hat{\vec{E}}$$
$$\hat{\vec{M}} = \mu_0 \frac{\omega_{pm}^2}{\omega_{m0}^2 - \omega^2 + i\Gamma_m \omega} \hat{\vec{H}}$$

These can be rearranged as

$$\begin{aligned} -\omega^2 \hat{\vec{P}} + i\Gamma_e \omega \hat{\vec{P}} + \omega_{e0}^2 \hat{\vec{P}} &= \varepsilon_0 \omega_{pe} \hat{\vec{E}} \\ -\omega^2 \hat{\vec{M}} + i\Gamma_m \omega \hat{\vec{M}} + \omega_{m0}^2 \hat{\vec{M}} &= \mu_0 \omega_{pm} \hat{\vec{H}} \end{aligned} \tag{5.28}$$

Performing an inverse Fourier transform, i.e. transforming $i\omega \to \frac{d}{dt}$ will then result in the time domain system for the dynamic evolution of $\vec{P}$ and $\vec{M}$

$$\begin{aligned} \frac{d^2\vec{P}}{dt^2} + \Gamma_e \frac{dP}{dt} + \omega_{e0}^2 \vec{P} &= \varepsilon_0 \omega_{pe} \vec{E}, \\ \frac{d^2\vec{M}}{dt^2} + \Gamma_m \frac{dM}{dt} + \omega_{m0}^2 \vec{M} &= \mu_0 \omega_{pm} \vec{H}. \end{aligned} \tag{5.29}$$

This system of ODEs are in in the 2$^{\text{nd}}$ order form for $\vec{P}$ and $\vec{M}$. By defining the polarization current density $\vec{J}$ and magnetization current density $\vec{K}$ we rewrite the ODEs in first order form as

$$\begin{aligned} \frac{\partial \vec{J}}{\partial t} + \Gamma_e \frac{dP}{dt} + \omega_{e0}^2 \vec{P} &= \varepsilon_0 \omega_{pe} \vec{E}, \\ \frac{\partial \vec{K}}{\partial t} + \Gamma_m \frac{dM}{dt} + \omega_{m0}^2 \vec{M} &= \mu_0 \omega_{pm} \vec{H}. \end{aligned} \tag{5.30}$$

The relationship between $\vec{J}$ and $\vec{P}$, and that of $\vec{K}$ & $\vec{M}$, can be explained by the third set of equations in (5.27), as $\frac{\partial \vec{P}}{\partial t} = \vec{J}$ and $\frac{\partial \vec{M}}{\partial t} = \vec{K}$.

Finally, the full system for the Lorentz Metamaterial in one dimension, performing a similar reduction to 1D as in the FEM in linear dielectrics, is then written as

$$\frac{1}{\varepsilon_0 \omega_{pe}^2}\frac{\partial J}{\partial t} + \frac{\Gamma_e}{\varepsilon_0 \omega_{pe}^2} J + \frac{\omega_{e0}^2}{\varepsilon_0 \omega_{pe}^2} P - E = 0, \tag{5.31a}$$

$$\varepsilon_0 \frac{\partial E}{\partial t} + J + \frac{\partial H}{\partial x} = 0, \tag{5.31b}$$

$$\frac{\partial P}{\partial t} = J. \tag{5.31c}$$

And for K and M,

$$\frac{1}{\mu_0 \omega_{pm}^2}\frac{\partial K}{\partial t} + \frac{\Gamma_m}{\mu_0 \omega_{pm}^2} K + \frac{\omega_{m0}^2}{\mu_0 \omega_{pm}^2} M - H = 0, \tag{5.32a}$$

$$\mu_0 \frac{\partial H}{\partial t} + K - \frac{\partial E}{\partial x} = 0, \tag{5.32b}$$

$$\frac{\partial M}{\partial t} = K. \tag{5.32c}$$

Then performing the variational formulation, integration by parts and matrix formulation in a manner similar to the FEM in linear dielectrics, we have

$$\frac{1}{\varepsilon_0 \omega_{pe}^2} M_E \frac{d}{dt}\vec{J}_h + \frac{\Gamma_e}{\varepsilon_0 \omega_{pe}^2} M_E \vec{J}_h + \frac{\omega_{e0}^2}{\varepsilon_0 \omega_{pe}^2} M_E \vec{P}_h - M_E \vec{E}_h = 0 \tag{5.33a}$$

$$\varepsilon_0 M_E \frac{d}{dt}\vec{E}_h + M_E \vec{J}_h - S H_h = 0 \tag{5.33b}$$

$$\frac{d}{dt}\vec{P}_h = \vec{J}_h \tag{5.33c}$$

$$\frac{1}{\mu_0 \omega_{pm}^2} M_H \frac{d}{dt}\vec{K}_h + \frac{\Gamma_m}{\mu_0 \omega_{pm}^2} M_H \vec{K}_h + \frac{\omega_{m0}^2}{\mu_0 \omega_{pm}^2} M_H \vec{M}_h - M_H H_h = 0 \tag{5.34a}$$

$$\mu_0 M_H \frac{d}{dt} H_h + M_H \vec{K}_h + S^T \vec{E}_h = 0 \tag{5.34b}$$

$$\frac{d}{dt}\vec{M}_h = \vec{K}_h \tag{5.34c}$$

With the vector fields of the form $\vec{F}_h$, where $F \in \{E, H, M, K, P, J\}$, are of the form

$$\vec{F}_h = [F_0, F_1, \ldots, F_N]^T \tag{5.35}$$

or, if on a staggered mesh,

$$\vec{F}_h = \left[F_{0+1/2}, F_{1+1/2}, \ldots, F_{N+1/2}\right]^T \tag{5.36}$$

The next step involves performing forward time discretizations on the $\frac{d}{dt}$ operators, and averaging terms for J in (5.33a) and for K in (5.34a). For brevity, the following constants are renamed:

$$\frac{1}{\varepsilon_0\omega_{pe}^2} = \alpha_e \qquad \frac{\Gamma_e}{\varepsilon_0\omega_{pe}^2} = \beta_e \qquad \frac{\omega_{e0}^2}{\varepsilon_0\omega_{pe}^2} = \gamma_e$$
$$\frac{1}{\mu_0\omega_{pm}^2} = \alpha_m \qquad \frac{\Gamma_m}{\mu_0\omega_{pm}^2} = \beta_m \qquad \frac{\omega_{m0}^2}{\mu_0\omega_{pm}^2} = \gamma_m$$

The last concept of note is, to preserve stability of the method, $\vec{J}_h$ and $\vec{K}_h$ are staggered in time with regards to the electric and magnetic fields' locations in time, respectively. The fully discrete scheme is given as

$$\alpha_e M_E \frac{\vec{J}_h^{n+3/2} - \vec{J}_h^{n+1/2}}{\Delta t} + \beta_e M_E \frac{\vec{J}_h^{n+3/2} + \vec{J}_h^{n+1/2}}{2} + \gamma_e M_E \vec{P}_h^{n+1} - M_E \vec{E}_h^{n+1} = 0, \tag{5.37a}$$

$$\varepsilon_0 M_E \frac{\vec{E}_h^{n+1} - \vec{E}_h^{n}}{\Delta t} + M_E \vec{J}_h^{n+1} - S\vec{H}_h^{n+1/2} = 0, \tag{5.37b}$$

$$\frac{\vec{P}_h^{n+1} - \vec{P}_h^{n}}{\Delta t} = \vec{J}_h^{n+1/2}. \tag{5.37c}$$

And

$$M_H \left(\alpha_m \frac{\vec{K}_h^{n+1} - \vec{K}_h^{n}}{\Delta t} + \beta_m \frac{\vec{K}_h^{n+1} - \vec{K}_h^{n}}{\Delta t} + \gamma_m \vec{M}_h^{n+1/2} - \vec{H}_h^{n+1/2} \right) = 0, \tag{5.38a}$$

$$\mu_0 M_H \frac{\vec{H}_h^{n+3/2} - \vec{H}_h^{n+1/2}}{\Delta t} + M_H \vec{H}_h^{n+1/2} + S^T \vec{E}_h^{n+1} = 0, \tag{5.38b}$$

$$\frac{\vec{M}_h^{n+3/2} - \vec{M}_h^{n+1/2}}{\Delta t} = \vec{K}_h^{n+1}. \tag{5.38c}$$

5.3 Construction of an Exact Solution

In this section, we construct an exact solution for system (5.27). We assume the following ansatz for E_y and H_z on the spatial domain $[0, 2\pi]$ and $\theta > 0$.

$$E(t, x) = E_0 e^{-\theta t} \sin kx \tag{5.39}$$

$$H(t, x) = H_0 e^{-\theta t} \cos kx \tag{5.40}$$

Our goal is to substitute these into equation (5.27). To begin, we need the derivatives with respect to x and with respect to t of E and H:

$$\frac{\partial E}{\partial x} = kE_0 e^{-\theta t}\cos kx, \qquad \frac{\partial \vec{E}}{\partial t} = -\theta E_0 e^{-\theta t}\sin kx, \tag{5.41}$$

$$\frac{\partial H}{\partial x} = -kH_0 e^{-\theta t}\sin kx, \qquad \frac{\partial \vec{H}}{\partial t} = -\theta H_0 e^{-\theta t}\cos kx. \tag{5.42}$$

Working with 5.31b first, we have

$$\varepsilon_0\left(-\theta E_0 e^{-\theta t}\sin(kx)\right) + J = kH_0 e^{-\theta t}\sin(kx) \tag{5.43}$$

this gives

$$J = e^{-\theta t}\sin(kx)\left(kH_0 + \varepsilon_0\theta E_0\right) \tag{5.44}$$

Now that we have an equation for $\vec{J}$ in terms of θ and k, we can substitute it into (5.31a) to solve for $\vec{P}$. First we find $\frac{\partial \vec{J}}{\partial t} = -\theta e^{-\theta t}\sin(kx)(kH_0 + \varepsilon_0\theta E_0)$. Then we have

$$-\theta e^{-\theta t}\sin(kx)(kH_0 + \varepsilon_0\theta E_0) + \Gamma_e e^{-\theta t}\sin(kx)\left(kH_0 + \varepsilon_0\theta E_0\right) + \omega_{e0}^2\vec{P} = \varepsilon_0\omega_{pe}^2 E_0 e^{-\theta t}\sin kx \tag{5.45}$$

Simplifying we get

$$\left(e^{-\theta t}\sin(kx)\right)\left(kH_0 + \varepsilon_0\theta E_0\right)\left(-\theta + \Gamma_e\right) + \omega_{e0}^2\vec{P} = \varepsilon_0\omega_{pe}^2 E_0\left(e^{-\theta t}\sin kx\right) \tag{5.46}$$

Finally we get

$$\vec{P} = \omega_{e0}^{-2}\left(e^{-\theta t}\sin(kx)\right)\left[\varepsilon_0\omega_{pe}^2 E_0 - \left(kH_0 + \varepsilon_0\theta E_0\right)\left(-\theta + \Gamma_e\right)\right] \tag{5.47}$$

Finally, we can then use our equations for $\vec{P}$ and $\vec{J}$ in 5.31c to get an expression for H_0 in terms of θ, k and E_0. First finding $\frac{\partial \vec{P}}{\partial t}$:

$$\frac{\partial \vec{P}}{\partial t} = -\omega_{e0}^{-2}\left(\theta e^{-\theta t}\sin(kx)\right)\left[\varepsilon_0\omega_{pe}^2 E_0 - \left(-kH_0 + \varepsilon_0\theta E_0\right)\left(-\theta + \Gamma_e\right)\right] \tag{5.48}$$

Then substituting into with equation (5.31c) we have

$$\left(-\theta\omega_{e0}^{-2}\right)\left(e^{-\theta t}\sin(kx)\right)\left(\varepsilon_0\omega_{pe}^2 E_0 - \left(\Gamma_m - \theta\right)\left(\varepsilon_0\theta E_0 + kH_0\right)\right) = \left(e^{-\theta t}\sin(kx)\right)\left(\varepsilon_0\theta E_0 + kH_0\right) \tag{5.49}$$

Simplifying,

$$E_0\left(-\theta\varepsilon_0\right)\left(\omega_{e0}^{-2}\omega_{pe}^2 - \theta\omega_{e0}^{-2}\left(\Gamma_e - \theta\right) + 1\right) = H_0 k\left(1 - \theta\omega_{e0}^{-2}\left(\Gamma_e - \theta\right)\right) \tag{5.50}$$

Solving for H_0,

$$H_0 = E_0 \frac{(-\theta\varepsilon_0)\left(\omega_{e0}^{-2}\omega_{pe}^2 - \theta\omega_{e0}^{-2}(\Gamma_e - \theta) + 1\right)}{k\left(1 - \theta\omega_{e0}^{-2}(\Gamma_e - \theta)\right)} \tag{5.51}$$

Now we work with the equations for H in order to get another equation for H_0 in terms of θ, k and E_0; starting with (5.32b):

$$\mu_0\left(-\theta H_0 e^{-\theta t}\cos kx\right) + \vec{K} = \left(kE_0 e^{-\theta t}\cos kx\right) \tag{5.52}$$

$$\vec{K} = \left(e^{-\theta t}\cos kx\right)(\mu_0\theta H_0 + kE_0) \tag{5.53}$$

Next working with (5.32a), needing $\frac{\partial\vec{K}}{\partial t} = -\theta\left(e^{-\theta t}\cos kx\right)(\mu_0\theta H_0 + kE_0)$:

$$(-\theta + \Gamma_m)\left(e^{-\theta t}\cos kx\right)(\mu_0\theta H_0 + kE_0) + \omega_{m0}^2\vec{M} = \mu_0\omega_{pm}^2 H_0\left(e^{-\theta t}\cos kx\right) \tag{5.54}$$

$$\vec{M} = \omega_{m0}^{-2}\left(e^{-\theta t}\cos kx\right)\left(\mu_0\omega_{pm}^2 H_0 - (-\theta + \Gamma_m)(\mu_0\theta H_0 + kE_0)\right) \tag{5.55}$$

Using this to solve 5.32c for our equation for H_0, with

$$\frac{\partial\vec{M}}{\partial t} = -\left(\theta\omega_{m0}^{-2}\right)\left(e^{-\theta t}\cos kx\right)\left(\mu_0\omega_{pm}^2 H_0 - (\Gamma_m - \theta)(\mu_0\theta H_0 + kE_0)\right) \tag{5.56}$$

Then we have

$$-\left(\theta\omega_{m0}^{-2}\right)\left(e^{-\theta t}\cos kx\right)\left(\mu_0\omega_{pm}^2 H_0 - (\Gamma_m - \theta)(\mu_0\theta H_0 + kE_0)\right) = \left(e^{-\theta t}\cos kx\right)(\mu_0\theta H_0 + kE_0) \tag{5.57}$$

$$H_0(\mu_0\theta)\left(-\omega_{m0}^{-2}\omega_{pm}^2 - \theta\omega_{m0}^{-2}(\Gamma_m - \theta) + 1\right) = E_0 k\left(1 - \theta\omega_{m0}^{-2}(\Gamma_m - \theta)\right) \tag{5.58}$$

$$H_0 = E_0\frac{k\left(1 - \theta\omega_{m0}^{-2}(\Gamma_m - \theta)\right)}{(-\mu_0\theta)\left(\omega_{m0}^{-2}\omega_{pm}^2 - \theta\omega_{m0}^{-2}(\Gamma_m - \theta) + 1\right)} \tag{5.59}$$

At this point, we can set our two equations for H_0 equal to each other to obtain a function for k in terms of θ.

$$\frac{k\left(1 - \theta\omega_{m0}^{-2}(\Gamma_m - \theta)\right)}{(-\mu_0\theta)\left(\omega_{m0}^{-2}\omega_{pm}^2 - \theta\omega_{m0}^{-2}(\Gamma_m - \theta) + 1\right)} = \frac{(-\theta\varepsilon_0)\left(\omega_{e0}^{-2}\omega_{pe}^2 - \theta\omega_{e0}^{-2}(\Gamma_e - \theta) + 1\right)}{k\left(1 - \theta\omega_{e0}^{-2}(\Gamma_e - \theta)\right)} \tag{5.60}$$

Cross multiply and combine like terms to get

$$k^2 = \theta^2\mu_0\varepsilon_0\frac{\theta^4 - \theta^3 A_{top} + \theta^2 B_{top} - \theta C_{top} + D_{top}}{\theta^4 - \theta^3 A_{bot} + \theta^2 B_{bot} - \theta C_{bot} + D_{bot}} \tag{5.61}$$

With the coefficients

$$\begin{aligned} A_{top} &= \Gamma_e + \Gamma_m & B_{top} &= \Gamma_e\Gamma_m + \omega_{pe}^2 + \omega_{e0}^2 + \omega_{pm}^2 + \omega_{m0}^2 \\ D_{top} &= \left(\omega_{pm}^2 + \omega_{m0}^2\right)\left(\omega_{e0}^2 + \omega_{pe}^2\right) & C_{top} &= \Gamma_m\left(\omega_{pe}^2 + \omega_{e0}^2\right) + \Gamma_e\left(\omega_{m0}^2 + \omega_{pm}^2\right) \\ A_{bot} &= \Gamma_e + \Gamma_m & B_{bot} &= \Gamma_e\Gamma_m + \omega_{m0}^2 + \omega_{e0}^2 \\ C_{bot} &= \omega_{e0}^2\Gamma_m + \omega_{m0}^2\Gamma_e & D_{bot} &= \omega_{e0}^2\omega_{m0}^2 \end{aligned}$$

This can be solved via Wolfram Mathematica (see Appendix) to get a value of θ for a chosen value of k, given certain experimental constants below:

$$\begin{aligned} \Gamma_e &= 2.5 & \varepsilon_0 &= 1 & \omega_{e0} &= 1 & \omega_{pe} &= 2 \\ \Gamma_m &= 2.5 & \mu_0 &= 1 & \omega_{m0} &= 1 & \omega_{pm} &= 2 \end{aligned}$$

Then numerically, for $k = 1$ the chosen value of θ is 0.142413. Using the previously calculated relationship between H_0 and E_0 in 5.59, choosing $E_0 = 1$, H_0 is calculated to be -0.571206. Then we have an exact solution for a sample wave to be

$$E(t,x) = e^{0.142413t}\sin x, \tag{5.62}$$
$$H(t,x) = -0.571206e^{0.142413t}\cos x, \tag{5.63}$$
$$J(t,x) = -0.713619e^{0.142413t}\sin x, \tag{5.64}$$
$$K(t,x) = -0.713619e^{0.142413t}\cos x, \tag{5.65}$$
$$P(t,x) = 2.114324e^{0.142413t}\sin x, \tag{5.66}$$
$$M(t,x) = -0.399148e^{0.142413t}\cos x. \tag{5.67}$$

5.4 Numerical Simulations for a Lorentz Metamaterial

This example will develop and demonstrate a Finite Element Method for Maxwell's equations in a Lorentz type metamaterial, with the exact solution given in section 5.3.

The first step between the equations in (5.38) and (5.37) and a coded example is rewriting them as iterative methods, as shown below:

$$\vec{J}_h^{\,n+3/2} = \left(\frac{\alpha_e}{\Delta t} + \frac{\beta_e}{2}\right)^{-1}\left(\vec{E}_h^{\,n+1} - \gamma_e\vec{P}_h^{\,n+1} - \left(\frac{\beta_e}{2} - \frac{\alpha_e}{\Delta t}\right)\vec{J}_h^{\,n+1/2}\right), \tag{5.68a}$$
$$\vec{E}_h^{\,n+1} = \vec{E}_h^{\,n} + \left(M_E^{-1}S\right)\frac{\Delta t}{\varepsilon_0}\vec{H}_h^{\,n-1/2}, \tag{5.68b}$$
$$\vec{P}_h^{\,n+1} = \vec{P}_h^{\,n} + \Delta t\vec{J}_h^{\,n+3/2}, \tag{5.68c}$$

$$\vec{K}_{h+1/2}^{\,n+3/2} = \left(\frac{\alpha_m}{\Delta t} + \frac{\beta_m}{2}\right)^{-1}, \left(\vec{H}_{h+1/2}^{\,n+1/2} - \vec{M}_{h+1/2}^{\,n+1/2} - \left(\frac{\beta_e}{2} - \frac{\alpha_e}{\Delta t}\right)\vec{K}_{h+1/2}^{\,n+1/2}\right), \tag{5.69a}$$

$$\vec{H}_{h+1/2}^{\,n+3/2} = \vec{H}_{h+1/2}^{\,n+1/2} - \frac{\Delta t}{\mu_0}\vec{K}_{h+1/2}^{\,n+1} - \left(M_H^{-1}S^T\right)\frac{\Delta t}{\mu_0}\vec{E}_h^{\,n+1}, \tag{5.69b}$$

$$\vec{M}_{h+1/2}^{\,n+3/2} = \vec{M}_{h+1/2}^{\,n+1/2} + \Delta t\vec{K}_{h+1/2}^{\,n+1}. \tag{5.69c}$$

With

$$\alpha_e = \frac{1}{\omega_{pe}^2\varepsilon_0} \quad \beta_e = \frac{\Gamma_e}{\omega_{pe}^2\varepsilon_0} \qquad \gamma_e = \frac{\omega_{e0}^2}{\omega_{pe}^2\varepsilon_0}$$

$$\alpha_m = \frac{1}{\omega_{pm}^2\mu_0} \quad \beta_m = \frac{\Gamma_m}{\omega_{pm}^2\mu_0} \quad \gamma_m = \frac{\omega_{m0}^2}{\omega_{pm}^2\mu_0}$$

A point worth noting is that of the matrix inverse product calculated in (5.68b) and (5.69b). The matrix M_H is the identity by our construction of the matrix, but the matrix M_E is tridiagonal, meaning its inverse is a full matrix. The result of this is that the product $(M_E^{-1}S)$ is very computationally expensive. Several methods can be taken to avoid this, chief among them an L-U factorization.

The next step to model the exact solution is to determine initial conditions, obtained from 5.39, 5.40, 5.44, 5.47, 5.53, and 5.55 evaluated with $t = 0$. Due to dependencies among time steps, the above six routines for updating their respective vectors in time must be run in the following order:

1. Calculate J (5.68a)
2. Calculate P (5.68c)
3. Calculate E (5.68b)
4. Ensure boundary conditions are appropriately reflected on E
5. Calculate K (5.69a)
6. Calculate M (5.69c)
7. Calculate H (5.69b)

The only step remaining is to iterate the above process for the desired number of time steps, choosing $\Delta t = 0.25 * h$ to satisfy stability conditions.

With a series of choices for $h = 0.0016, 0.0008, 0.0004, 0.0002, 0.0001$, convergence is shown by the ratio between the errors at successively halved time steps. After 500 time steps (such that $t = 500\Delta t$), the following figures are plots of the exact and approximate electric field, magnetic field, polarization field and magnetization field are plotted in figures 5.1 and 5.2.

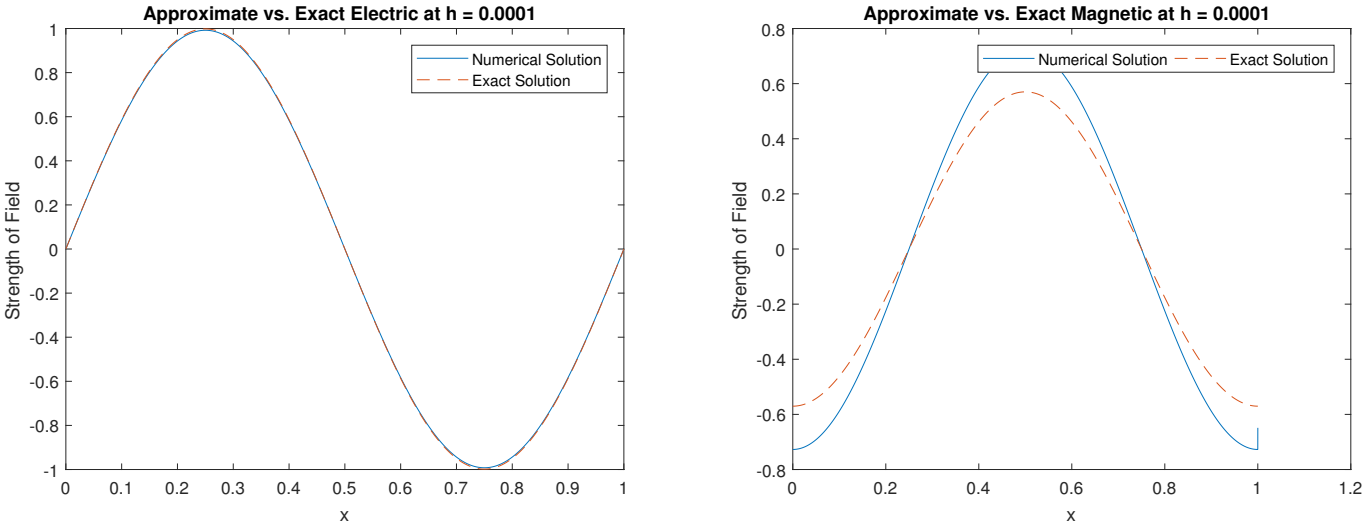

Figure 5.1: Differences between approximate and exact electric and magnetic fields for $h = 0.0016$ or $h = 0.0001$. The exact field is given as a dashed red line, and the approximate field is graphed as a solid blue line.

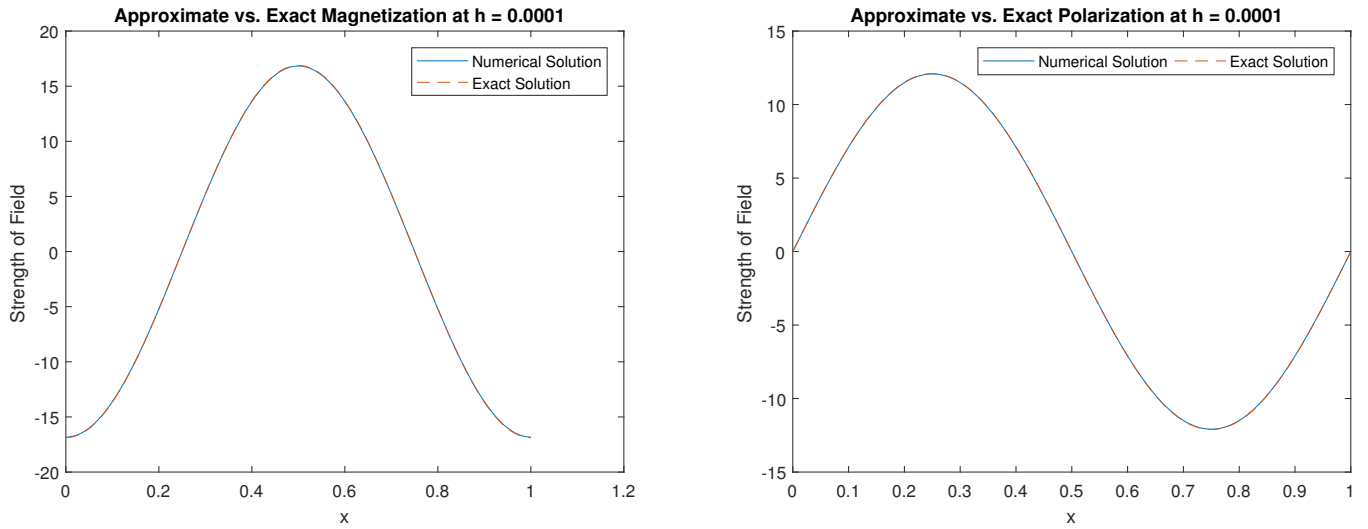

Figure 5.2: Approximate and exact magnetization and polarization fields for $h = 0.0001$. The exact field is given as a dashed red line, and the approximate field is graphed as a solid blue line.

The error in each of the four fields in question can be found in tables 5.2 - 5.5 for $h = 0.0016, 0.0008, 0.0004, 0.0002, 0.0001$. The error for the field F was calculated by

$$\mathcal{E}_F(t) = \sqrt{h \sum_{k=0}^{N} (F_k - \mathcal{F}_k)^2} \tag{5.70}$$

with N the total number of step sizes $1/h$ and $\mathcal{F}_k$ the exact solution to the field in question at the node k at time $t = 500\Delta t$.

In the case of the electric field, the ratio between the error at step size h and at step size $h/2$ approaches 4, meaning that the method is second order accurate in approximating the electric field. This can be seen in the Ratio column of Figure 5.2 and in the slope of Table 5.3.

For the magnetic field, polarization and magnetization, the ratio of successive step size's errors approaches 2, meaning that the method is first order accurate in approximating the magnetic, polarization and magnetization fields. This can be seen in Figures 5.3 - 5.6.

Step Size	Error (Electric)	Ratio
0.0016	0.94556	-
0.0008	0.26773	3.5317671
0.0004	0.069107	3.8741372
0.0002	0.017426	3.9657408
0.0001	0.0043682	3.9892862

Table 5.2: Error between the exact and approximate electric field at $t = 500$. The ratio column gives the ratio between the previous step size's error and the current step size's error; the ratio converges to 4, implying that the method is second order accurate in the electric field.

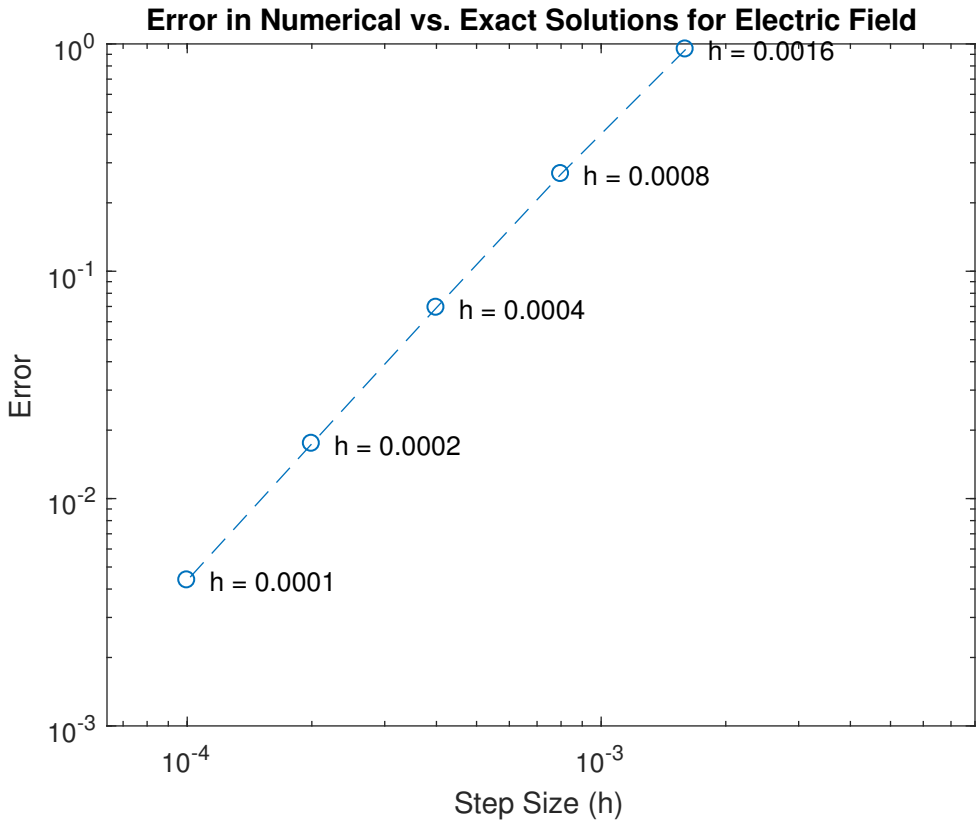

Figure 5.3: Error in numerical versus exact solutions for electric field in a Lorentz metamaterial. Graph nodes are labeled with the step size that accompanies the point. As the step size halves, the error quarters, implying the method is second order accurate when calculating the electric field.

Step Size	Error (Magnetic)	Ratio
0.0016	1.28970	-
0.0008	0.82106	1.5707743
0.0004	0.43556	1.8850675
0.0002	0.22118	1.9692558
0.0001	0.11107	1.9913568

Table 5.3: Error between the exact and approximate magnetic field at $t = 500$. The ratio column gives the ratio between the previous step size's error and the current step size's error; the ratio converges to 2, implying that the method is first order accurate in the magnetic field.

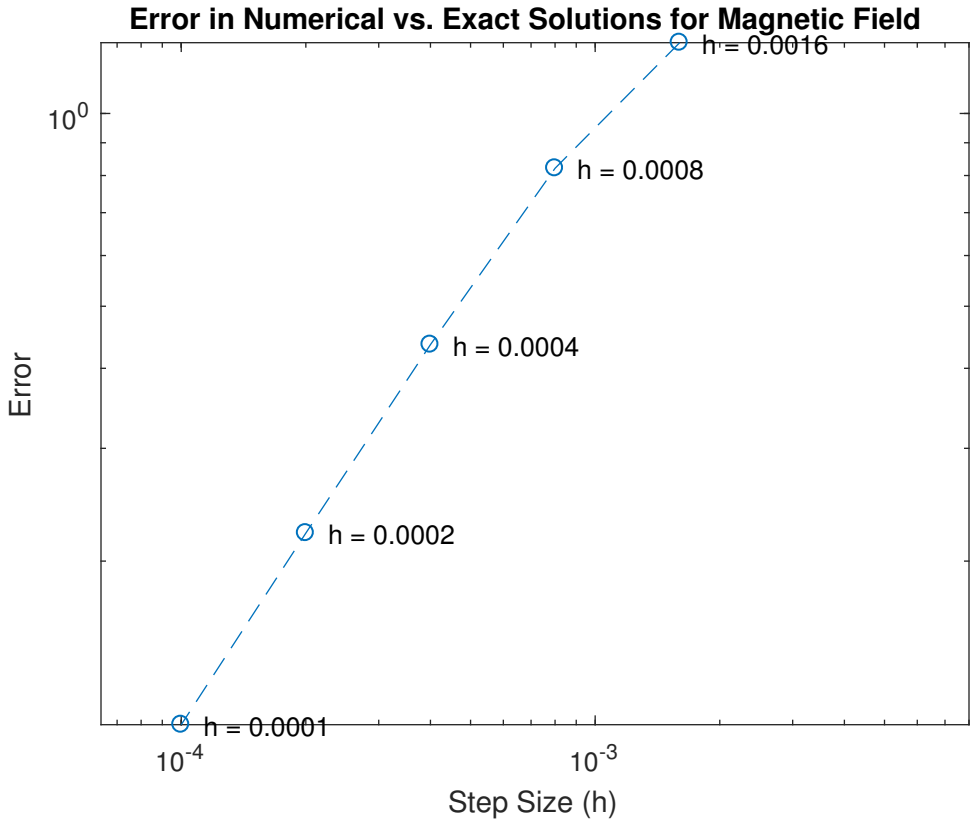

Figure 5.4: Error in numerical versus exact solutions for magnetic field in a Lorentz metamaterial. Graph nodes are labeled with the step size that accompanies the point. As the step size halves, the error halves as well, implying the method is first order accurate for the magnetic field.

Step Size	Error(Polarization)	Ratio
0.0016	0.251920	-
0.0008	0.121900	2.066612
0.0004	0.060859	2.002991
0.0002	0.030469	1.997407
0.0001	0.015248	1.998229

Table 5.4: Error between the exact and approximate polarization field at $t = 500$. The ratio column gives the ratio between the previous step size's error and the current step size's error; the ratio converges to 2, implying that the method is first order accurate in the polarization field.

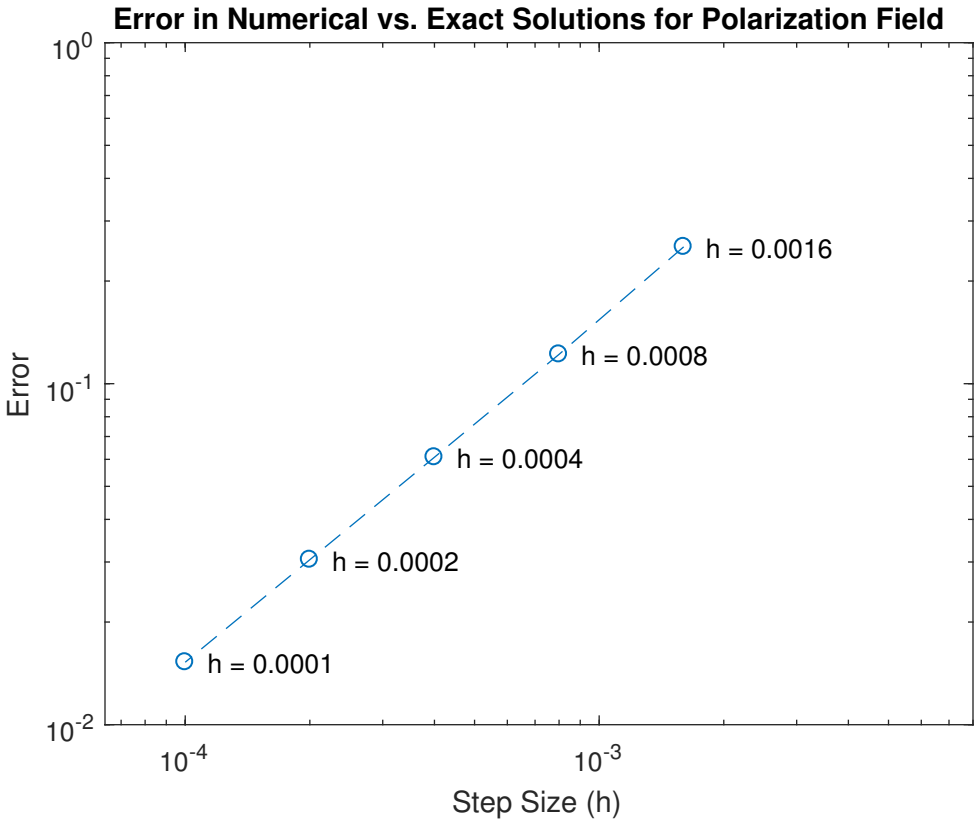

Figure 5.5: Error in numerical versus exact solutions for polarization field in a Lorentz metamaterial. Graph nodes are labeled with the step size that accompanies the point. As the step size halves, the error halves as well, implying the method is first order accurate for the Polarization field.

Step Size	Error (Magnetization)	Ratio
0.0016	0.49015	-
0.0008	0.26158	1.8738053
0.0004	0.13338	1.9611635
0.0002	0.067086	1.9881942
0.0001	0.033607	1.9961913

Table 5.5: Error between the exact and approximate magnetization field at $t = 500$. The ratio column gives the ratio between the previous step size's error and the current step size's error; the ratio converges to 2, implying that the method is first order accurate in the electric field.

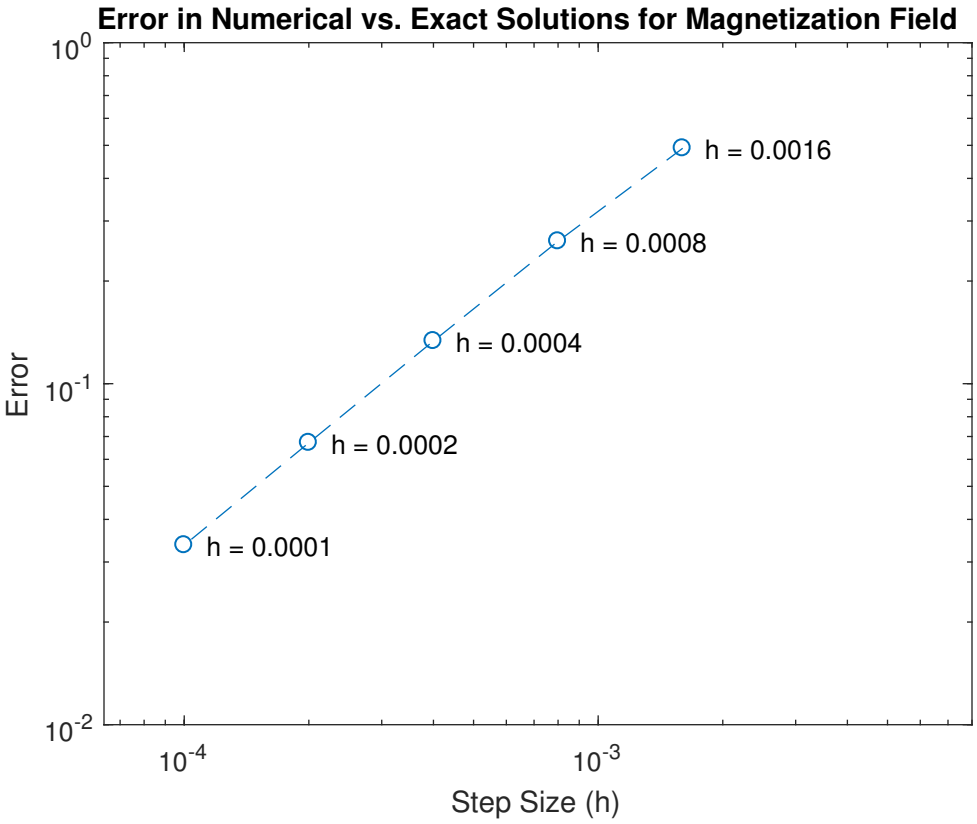

Figure 5.6: Error in numerical versus exact solutions for magnetization field in a Lorentz metamaterial. Graph nodes are labeled with the step size that accompanies the point. As the step size halves, the error halves as well, implying the method is first order accurate for the magnetization field.

6 Discussion and Conclusions

In this thesis, finite difference and finite element methods are presented for Maxwell's equations in one spatial dimension and in both linear dielectrics and a Lorentz-type metamaterial. Initially, finite difference methods are presented, and two numerical simulations are presented of a sinusoidal wave in periodic boundary conditions and the propagation of a Gaussian pulse with reflecting boundary conditions. Finite element methods for Maxwell's equations are presented next, and a numerical simulation is presented for the same boundary value problem as in the finite difference section.

Finally, Maxwell's equations in linear metamaterials are presented, and an exact solution is developed for a Lorentz metamaterial. A finite element method that is second order in time for the electric field and first order in time for the magnetic, polarization and magnetization fields is presented, and a numerical simulation is performed and compared to the exact solution developed in the thesis. The main result of this thesis is the development of the finite element method for the Lorentz metamaterial and its numerical implementation.

7 Appendix: Matlab Code

7.1 1-D Yee Scheme with Periodic Boundary Conditions

```
%1-D Yee scheme for simulating propagation of sine wave in periodic
%boundary conditions
a = 0;
b = 2*pi; %space goes from a->b, or 0->2*pi
TMAX = 20*pi; %time goes from 0 -> 20*pi

Error = [];
E_exact = @(x,t)(sin(x+t))';

for Ns = 2.^(3:9) %number of spatial points
        %set up spatial parameters
        h = b/Ns;
        prim = a:h:b;
        stag = (a+h/2):h:(b-h/2);

        %set up temporal parameters
        dt = h/2;
        Nt = TMAX/dt; %number of temporal points

        %declare electric and magnetic arrays
        E = zeros(Ns+1,1);
        Eprev = sin(prim)';

        H = zeros(Ns,1);
        Hprev = sin(stag)';

        %main time step loop!
        for t = 1:Nt
                %calc new E vector, correcting for periodic BC @ endpoints
                E(1) = Eprev(1) - (dt/h)*(Hprev(1) - Hprev(Ns));
                for j = 2:Ns
                        E(j) = Eprev(j) - (dt/h)*(Hprev(j) - Hprev(j-1));
                end
                E(Ns+1) = E(1);

                %calc new H vector
                for k = 1:Ns
```

```
38                          H(k) = Hprev(k) - (dt/h)*(E(k+1) - E(k));
39                  end
40
41                  %correct previous time step vectors
42                  Eprev = E;
43                  Hprev = H;
44          end
45
46
47          x = 0:Ns;
48          %clf;
49          figure();
50          plot(x,E,x,sin(0:h:2*pi));
51          xlabel('y');
52          ylabel('Electric Field');
53          title(['Numerical vs. Exact Electric Field at Tmax with Ns
                = ' num2str(Ns)])
54          %pause;
55          %close(1);
56
57          Error = [Error sqrt(h*sum( (E - E_exact(prim,TMAX)) .^2))
                ];
58
59  end
60  %ratios of successive errors
61  ratios = Error(1:length(Error)-1)./Error(2:length(Error));
62  %plot table of errors including error ratios
63  T = table(pi* (2.^-(3:9)'),Error',[0 ratios]')
64
65  %log-log plot of step size vs. error
66  %clf;
67  %figure(1);
68  dom = 2.^(3:9);
69  loglog(dom,Error,'o-');
70  % xlim([5 600]);
71  xlabel('log(Ns)');
72  ylabel('log(Error)');
73  title('Error in Numerical vs. Exact Solutions');
74  for j = 1:length(dom)
75          text(dom(j)-dom(j)/10,Error(j)-Error(j)/10,[ ' Ns = '
              num2str(dom(j))],'HorizontalAlignment','right');
76  end
77  %pause
```

7.2 1-D Yee Scheme Gaussian Pulse Approximation

```
%1-D Finite Difference Yee Scheme

SPACE_STEPS = 200;  %number of segments the boundary 0,1 has been
    parsed into
TIME_STEPS  = 2000; %amount of time loop iterations to run

E_ARRAY = zeros(1, SPACE_STEPS); %contains electric field data
H_ARRAY = zeros(1, SPACE_STEPS); %contains magnetic field data

center_of_pulse = 40; %gaussian pulse peaks at this time

current_time = 0; %keeps track of current time step

C = 1;
QUOTIENT = 0.5;
%QUOTIENT = C*(delta_t / delta_h);
%represents delta t / c*delta x; is less than one thus
%stability conditions are met

SPREAD = 12; %"spread" of gaussian pulse.
%increasing this value degrades the behavior of the wave; why is
    this?

for i = 1:TIME_STEPS %loop iterates through time

        %keep track of the current time
        current_time = current_time + 1;

        %iterate through electric field, omitting boundaries
        for j = 2:SPACE_STEPS-1
                %standard yee scheme:
                %E@(n+1,j) = E@(n,j) + 0.5*(H@(N+0.5,J+0.5) - H@(N
                    +0.5,J-0.5))
                E_ARRAY(j) = E_ARRAY(j) + (QUOTIENT)*(H_ARRAY(j+1)
                    - H_ARRAY(j));
        end

        %set the middle of the spatial domain to model the
            formation of
        %gaussian pulse that peaks at t=40.
        E_ARRAY((SPACE_STEPS/2)) = E_ARRAY((SPACE_STEPS/2)) + exp
            (-.5*((center_of_pulse - current_time)/SPREAD)^2);

```

```
38          %similar yee iteration for magnetic field
39          for j = 2:SPACE_STEPS
40                  H_ARRAY(j) = H_ARRAY(j) + (QUOTIENT)*(E_ARRAY(j) -
                        E_ARRAY(j-1));
41          end
42
43          %zeros(1:SPACE_STEPS) runs out of memory so this is a work
                -around
44          zlimits = 1:SPACE_STEPS;
45          for k = 1:SPACE_STEPS
46                  zlimits(k) = 0;
47          end
48
49          %if the current time step is divisible by 5, plot it
50          %this is to reduce the number of times the user must press
                key to continue
51          if mod(current_time,5) == 0
52          %plot the electric and magnetic fields together (purely
                for show;
53          %this is in no way a reflection of the actual physical
                properties
54          %of the system)
55
56          plot3(1:SPACE_STEPS,E_ARRAY,zlimits,1:SPACE_STEPS,zlimits,
                H_ARRAY); %plot the electric field array
57          xlim([0 200])
58          ylim([-2 2])
59          zlim([-2 2])
60          title(['EM Fields @ t=' num2str(current_time) '; Press any
                key to continue'],'HandleVisibility','off');
61
62          %thie following three lines of code ensure that when the
                next set
63          %of data is plotted on the same axis, the previous plot is
64          %overwritten (to greatly reduce noise and make the graph
                readable)
65          ylabel('Y','HandleVisibility','off');
66          xlabel('X','HandleVisibility','off');
67          set(gca,'NextPlot','replacechildren') ;
68
69          %after plotting, wait for user to press any key (or mouse
                button)
70          %to continue
71          WAIT = waitforbuttonpress;
72          end
```

```
73
74 end %end of time-based loop
```

7.3 1-D Finite Element Simulation in a Linear Dielectric

```
%1-D Yee scheme for simulating propagation of sine wave in
    periodic
%boundary conditions
a = 0;
b = 2*pi; %space goes from a->b, or 0->2*pi
TMAX = 20*pi; %time goes from 0 -> 20*pi

Error = [];
E_exact = @(x,t)(sin(x+t))';

for Ns = 2.^(3:9) %number of spatial points
%set up spatial parameters
h = b/Ns;
prim = a:h:b;
stag = (a+h/2):h:(b-h/2);

%set up temporal parameters
dt = h/2;
Nt = TMAX/dt; %number of temporal points

%declare electric and magnetic arrays
E = zeros(Ns+1,1);
Eprev = sin(prim)';

H = zeros(Ns,1);
Hprev = sin(stag)';

%main time step loop!
for t = 1:Nt
%calc new E vector, correcting for periodic BC @ endpoints
E(1) = Eprev(1) - (dt/h)*(Hprev(1) - Hprev(Ns));
for j = 2:Ns
E(j) = Eprev(j) - (dt/h)*(Hprev(j) - Hprev(j-1));
end
E(Ns+1) = E(1);

%calc new H vector
for k = 1:Ns
H(k) = Hprev(k) - (dt/h)*(E(k+1) - E(k));
end

%correct previous time step vectors
Eprev = E;
```

```
43 Hprev = H;
44 end
45
46
47 x = 0:Ns;
48 %clf;
49 eFig = figure;
50 set(eFig, 'Position', [500, 500, 450, 300]);
51 plot(x,E,x,sin(0:h:2*pi));
52 xlabel('y');
53 ylabel('Electric Field');
54 title(['Numerical vs. Exact Electric Field at Tmax'])
55 legend('Exact Solution','Numerical Solution','Location','northeast
     ','Orientation','horizontal');
56 %pause;
57 %close(1);
58
59 Error = [Error sqrt(h*sum( (E - E_exact(prim,TMAX)) .^2))];
60
61 end
62 %ratios of successive errors
63 ratios = Error(1:length(Error)-1)./Error(2:length(Error));
64 %plot table of errors including error ratios
65 T = table(pi* (2.^-(3:9)'),Error',[0 ratios]')
66
67 %log-log plot of step size vs. error
68 %clf;
69 %figure(1);
70 figure;
71 dom = 2.^(3:9);
72 loglog(dom,Error,'o-');
73 % xlim([5 600]);
74 xlabel('log(Ns)');
75 ylabel('log(Error)');
76 title('Error in Numerical vs. Exact Solutions');
77 for j = 1:length(dom)
78 text(dom(j)-dom(j)/10,Error(j)-Error(j)/10,[ ' Ns = ' num2str(dom(
     j))],'HorizontalAlignment','right');
79 end
```

7.4 Mathematica Code for an Exact Solution for the Lorentz Metamaterial Model

The following is code in the Wolfram Mathematica language used to calculate the values of θ and H_0 in the exact solution to the Lorentz material.

First, set the constants:

$\Gamma_e = 1/0.4$

$\Gamma_m = 1/0.4$

$\mu_0 = 1$

$\epsilon_0 = 1$

$\omega_{m0} = 1$

$\omega_{e0} = 1$

$\omega_{pm} = 2$

$\omega_{pe} = 2$

$H0[x\_] := 1 * \frac{\epsilon_0 x(\omega_{e0} x(\Gamma_e - x) - (\omega_{e0}\text{^}-1)\omega_{pe} - 1)}{1(1 - x(\omega_{e0}\text{^}-1)(\Gamma_e - x))}$

Then, declare the appropriate algebraic combinations of constants from the derivation of exact solution:

$a = \Gamma_e + \Gamma_m$

$b = \Gamma_e \Gamma_m + \omega_{pe}\text{^}2 + \omega_{m0}\text{^}2 + \omega_{e0}\text{^}2 + \omega_{pm}\text{^}2$

$c = \Gamma_m (\omega_{pe}\text{^}2 + \omega_{e0}\text{^}2) + \Gamma_e (\omega_{pm}\text{^}2 + \omega_{m0}\text{^}2)$

$d = (\omega_{e0}\text{^}2 + \omega_{pe}\text{^}2)(\omega_{m0}\text{^}2 + \omega_{pm}\text{^}2)$

$f = \Gamma_e \Gamma_m + \omega_{m0}\text{^}2 + \omega_{e0}\text{^}2$

$g = \omega_{e0}\text{^}2 \Gamma_m + \omega_{m0}\text{^}2 \Gamma_e$

$h = \omega_{e0}\text{^}2 \omega_{m0}\text{^}2$

$k = \mu_0 \epsilon_0$

Finally, solve the rational function for θ (here represented as x):

$$\text{NSolve}[k * (x\text{^}6 - (a)x\text{^}5 + (b)x\text{^}4 - (c)x\text{^}3 + (d)x\text{^}2)/(x\text{^}4 \ - (a)x\text{^}3 + (f)x\text{^}2 - (g)x + h) == 1, x]$$

$$\{\{x \to \text{“1.67879”} \ - \text{“2.05024”}\, i\}, \{x \to \text{“1.67879”} \ + \text{“2.05024”}\, i\}, \{x \to \text{“0.911805”} \ - \text{“1.50291”}\, i\},$$
$$\{x \to \text{“0.911805”} \ + \text{“1.50291”}\, i\}, \{x \to -\text{“0.32361”}\}, \{x \to \text{“0.142413”}\}\}$$

Checking answer by plugging in 0.142413:

$$\text{Function}\left[x, \frac{k\left(x^6 - a x^5 + b x^4 - c x^3 + d x^2\right)}{x^4 - a x^3 + f x^2 - g x + h}\right][\text{“0.142413”}]$$

1.

This is the desired result. Finally, solve for $H0$:

$$\text{H0}[\text{“0.142413”}]$$

-0.571206

7.5 1D Finite Element Simulation in a Lorentz Metamaterial

```
%1D code for wave propagation in lorentz metamaterial using FEM
%Warning: this code takes approximately 10 minutes to run on the
   author's
%machine with all step sizes enabled.
clear all;
theta = 0.14241288955782322;
E0 = 1;
H0 = -0.571206;
k = 2*pi;
%set up meshes
stepsizes = [1/625 1/1250 1/2500 1/5000 1/10000];
eError = []; jError = []; pError = [];
hError = []; kError = []; mError = [];
tic
for h = stepsizes
        mesh = 0:h:1;
        stag = (h/2):h:(1+h/2);
        %satisfy CFL condition
        dt = 0.25*h;

        S = Gstiff(mesh); %stiffness matrix
        Me = h*GmassElec(mesh);
        Mm = h*eye(length(stag));

        %set up initial conditions for vectors:
        E = Eexact(mesh,0,k,theta,E0)';
        P = PExact(mesh,0,k,theta,E0,H0,1,1,2,2.5)';
        J = JExact(mesh,0,k,theta,E0,H0,1)';

        H = Hexact(stag,0,k,theta,H0)';
        K = KExact(stag,0,k,theta,E0,H0,1)';
        M = MExact(stag,0,k,theta,E0,H0,1,1,2,2.5)';

        %iterate for 500 time steps
        tmax = 500;

        A = (Me\S');
        B = (Mm\S);
        for n = 0:tmax
                J = ((3.2*dt)/(dt + 0.8))*(E - 0.25*P - (0.3125 -
                   (1/(4*dt)))*J);
                P = P + dt*J;
                E = E - (dt)*J + (dt)*A*H;
```

```
42                 %enforce zero boundary conditions
43                 E(1) = 0;
44                 E(length(mesh)) = 0;
45                 K = ((3.2*dt)/(dt + 0.8))*(H - 0.25*M - (0.3125 -
                       (1/(4*dt)))*K);
46                 M = M + dt*K;
47                 H = H - dt*K - dt*B*E;
48           end
49           figure;
50           if h == 1/625 || h == 1/10000 %on first and last time step
                 , plot all fields to make sure we're actually getting
                 better
51                 plot(mesh,E',mesh,Eexact(mesh,n*dt,k,theta,E0),'--
                       ');
52                 title(['Approximate vs. Exact Electric at h = '
                       num2str(h)])
53                 xlabel('x')
54                 ylabel('Strength of Field')
55                 legend('Numerical Solution','Exact Solution','
                       Location','northeast','Orientation','horizontal
                       ');
56                 figure;
57                 plot(stag,H',stag,Hexact(stag,n*dt,k,theta,H0),'--
                       ');
58                 title(['Approximate vs. Exact Magnetic at h = '
                       num2str(h)])
59                 xlabel('x')
60                 ylabel('Strength of Field')
61                 legend('Numerical Solution','Exact Solution','
                       Location','northeast','Orientation','horizontal
                       ');
62                 figure;
63                 plot(mesh,P',mesh,PExact(mesh,n*dt,k,theta,E0,H0
                       ,1,1,2,2.5),'--');
64                 title(['Approximate vs. Exact Polarization at h =
                       ' num2str(h)])
65                 xlabel('x')
66                 ylabel('Strength of Field')
67                 legend('Numerical Solution','Exact Solution','
                       Location','northeast','Orientation','horizontal
                       ');
68                 figure;
69                 plot(stag,M',stag,MExact(stag,n*dt,k,theta,E0,H0
                       ,1,1,2,2.5),'--');
70                 title(['Approximate vs. Exact Magnetization at h =
```

```
                    ' num2str(h)])
71                  xlabel('x')
72                  ylabel('Strength of Field')
73                  legend('Numerical Solution','Exact Solution','
                        Location','northeast','Orientation','horizontal
                        ');
74          end
75          eError = [eError sqrt(h*sum((E - Eexact(mesh,n*dt,k,theta,
                E0)').^2))];
76          hError = [hError sqrt(h*sum((H - Hexact(stag,n*dt,k,theta,
                H0)').^2))];
77          pError = [pError sqrt(h*sum((P - PExact(mesh,n*dt,k,theta,
                E0,H0,1,1,2,2.5)').^2))];
78          jError = [jError sqrt(h*sum((J - JExact(mesh,n*dt,k,theta,
                E0,H0,1)').^2))];
79          kError = [kError sqrt(h*sum((K - KExact(stag,n*dt,k,theta,
                E0,H0,1)').^2))];
80          mError = [mError sqrt(h*sum((M - MExact(stag,n*dt,k,theta,
                E0,H0,1,1,2,2.5)').^2))];
81          toc
82  end
83  ErrorGraph(stepsizes,eError,'Electric');
84  ErrorGraph(stepsizes,hError,'Magnetic');
85  ErrorGraph(stepsizes,pError,'Polarization');
86  ErrorGraph(stepsizes,mError,'Magnetization');
87  %these tables can be displayed by deleteing the semicolon at the
        end of
88  %each line
89  Te = table(stepsizes',eError');
90  Th = table(stepsizes',hError');
91  Tp = table(stepsizes',pError');
92  Tm = table(stepsizes',mError');
```

References

[1] F. Bilotti and L. Sevgi, *Metamaterials: Definitions, properties, applications, and fdtd-based modeling and simulation*, International Journal of RF and Microwave Computer-Aided Engineering, 22 (2012), pp. 422–438.

[2] J. Li and Y. Huang, *Time-domain finite element methods for Maxwell's equations in metamaterials*, vol. 43, Springer Science & Business Media, 2012.

[3] J. Maxwell, *On faraday's lines of force*, Transactions of the Cambridge Philosophical Society, 10 (1864), p. 27.

[4] T. Rylander, P. Ingelström, and A. Bondeson, *Computational electromagnetics*, Springer Science & Business Media, 2012.

[5] D. Smith, W. Padilla, D. Vier, S. Nemat-Nasser, and S. Schultz, *Composite medium with simultaneously negative permeability and permittivity*, Physical review letters, 84 (2000), p. 4184.

[6] D. Sullivan, *Electromagnetic simulation using the FDTD method*, John Wiley & Sons, 2013.